7-2021

Grid Strength Assessment Trough Q-V Modal Analysis and Maximum Loadability of a Wind-Dominated Power System Using P-Q Regions

Pierre Obed Dorile
University of Arkansas, Fayetteville

Grid Strength Assessment Trough Q-V Modal Analysis and Maximum Loadability of a Wind-Dominated Power System Using P-Q Regions

A thesis submitted in partial fulfillment
of the requirements for the degree of
Master of Science in Electrical Engineering

by

Pierre Obed Dorile
The University Of the West Indies, Saint Augustine Campus
Bachelor of Engineering in Electrical Engineering

July 2021
University of Arkansas

This dissertation is approved for recommendation to the Graduate Council.

Roy McCann PhD
Thesis Director:

Fang Luo PhD
Committee member

Jingxian Wu PhD
Committee member

Abstract

Climate change is a menace to the existence of the world and policymakers are trying to tackle this phenomenon by deploying large-scale wind farms into their grids. Among them, wind energy shows a promising future to substitute the traditional power plants. However, the deployment of these wind farms into the grid is not a panacea that does not pose any challenges to the grid operators. Keeping the power system voltage stable while considering the strength of the transmission grid is among the major challenges facing by the transmission system operators. Amid normal operation and fault conditions, wind farms should help the grid in reactive power supply according to the grid codes to ride through the fault. In doing so, during fault conditions or heavy loading conditions, the voltage of the power system will not deteriorate. A wind farm, most of the time, is incapable to meet the grid codes requirements without reactive power support. For the compensation of the reactive power deficit, FACTS devices are extensively used. The most popular FACTS devices used by electric utilities are, STATCOM, SVC, SSSC, TCSC, and UPFC. In this work, attention is given to the amelioration of transient stability in wind-dominated power systems via STATCOM and SSSC. Furthermore, a systematic approach to locate large wind power plants to an existing transmission grid is developed by combining the QV-modal analysis, Q-V curves, and P-Q method. The steady-state voltage stability at different wind power penetration levels is investigated while considering the weakest and the strongest region of the power system. The P-Q region method is used to size the wind farm in each scenario. The reliability of the system is verified from the worst contingencies with the wind farm connected at the most vulnerable bus of the system in reactive power capability. The system considered for testing is the modified IEEE 14 bus system.

Acknowledgment

Firstly, my sincerest appreciation and gratitude goes to my advisor Dr. McCann, one of the finest in power system at the University of Arkansas, for his guidance and support during my research at his group. Many thanks Dr. for your unselfish help and priceless support amid the completion of my thesis under your guidance. You have impressed me by working with you for your broad knowledge in the realm of power systems from theoretical and practical standpoints. Also, I want to thank my dissertation committee members, Dr. Jingxian Wu and Dr. Fang Luo for serving on the committee.

Apart from my advisor, wholehearted thanks go to my teammates at the power system control laboratory, Mojtaba, Desmon, Ahmed, and Rajiv for their discussions and constructive feedback throughout my research. They are among the brightest students that I have ever met throughout my studies at the University of Arkansas. Also, I express endlessly my thanks to my family and parents for their love and support. Without you, this would have never been possible. I enjoyed my stay at the University of Arkansas, Fayetteville. Special thanks goes to Carina Hoffmann who provides to me fro free the student version of the powerful software DigSILENT PowerFactory.

Last but never the least, I would thank the Great Architect of the Universe for providing me the mental and physical strength to complete my course study and the thesis on time.

Contents

List of Figures

List of Tables

Chapter 1

Introduction

This section highlights the problem statement followed by a brief description of current global challenges on this topic is mentioned and quick statement of the proposed solution are provided.

1.1 Overview

The climate change phenomenon is menacing the existence of the world. Policymakers worldwide are busy trying to cope with this phenomenon by integrating a huge amount of renewable energy into their transmission grids. Wind energy offers a great alternative to the use of fossil fuels for electrical energy generation. According to [1],[7] 23.7% of the total electricity worldwide comes from hydro-power. In some countries like Germany, Denmark, Spain, the wind power market penetration is extremely high. Indeed, in Europe, 15.6% of the total installed capacity is wind energy [1],[2],[7]. However, one must keep in mind that wind energy is not a cure-all remedy and can pose several challenges to grid operators and system planners. In a traditional power system, synchronous machines are widely used to generate electrical power. These machines, by their inherent properties, are amazing. However, in the last decades, the landscape of the power industry is under tremendous changes since increased wind energy is being integrated into the transmission grid. Wind energy by its nature is intermittent and has limited predictability. To generate power, wind turbines used induction generators and power electronics converters which have low inertia. The long transmission line that evacuates the power from the wind park consumes a lot of reactive power; consequently, they are weak. Also, the replacement of the traditional synchronous machines with power-electronics-based converters has several drawbacks on the reliable operations of the transmission grid. For these

reasons, it is more than necessary to research the consequences of these power electronics-based generators on the dynamic and static behavior of the wind-dominated power system. Researchers and scholars in the literature of power systems such as [3],[4] state that wind power generation affects system stability like voltage stability. I n [5], power is voltage stable if it can keep an acceptable voltage at its buses following a major disturbance. Maintaining these wind farms online during fault conditions is crucial to the transmission system. Wind turbines should be able to stay online under transient voltage conditions per grid code requirements [2]. Transmission systems operators have set the so-called grid code requirements that need to be met such that these wind farms could stay online during a fault condition from the transmission grid. Most of the time, the integration of these wind farms does not necessitate considerable alteration of the existing transmission system; however, a sophisticated technical analysis needs to be carried out before the interconnection. The effects of these wind parks need to be researched to come up with a feasible technical solution to mitigate the negative impacts on the stability of the grid. Also, the deployment of these wind farms reduces the reactive power capability of the traditional power system. The power system planners need to carry out careful analysis before integrating these wind farms into the grid. The weakest and strongest area of the power system needs to be identified to reliably operate the power system. PV curves and QV curves are combined to assess the maximum loading conditions of the transmission grid. These curves can be derived without requiring a lot of computational time. FACTS equipment can help in the amelioration of the transient stability since they can inject reactive during fault conditions from the external grid. Moreover, they can help in the augmentation of the transfer margin of the transmission grid. Additionally, the maximum loadability of the wind-dominated power, in this work, is under investigation during the normal operation and during the worst contingencies. The P-Q region method is used for this purpose.

1.2 Problem Motivation

With the deployment of more and more wind farms into the modern power system, it is crucial to assess how much wind that can be integrated safely and reliably without harming the voltage stability and frequency stability is a complex question. Generally, the limiting factors are the size of the wind farm and the strength of the power system. Also, the type of wind turbines types plays a major role in the stability of the system. Indeed, most modern wind turbines can assist the transmission grid in terms of reactive power demand in needy time. Thus, it is imperative to develop well-formulated and organized approaches to optimize the wind power injection into a weak power system. After all, these methods and procedures can be used by planning engineers in maximizing wind penetration levels. Also, it is wise to research the optimal wind farm sizes in a weak power system considering the available reactive power without performing wind power curtailment. Furthermore, is necessary to come up with methods for locating FACTS devices like STATCOM, SSSC, SVC to help in the augmentation in the wind penetration levels.

1.3 Thesis Outline

The integration of Renewable Energy Resources is expanding rapidly throughout the world due to environmental concerns to come up with cleaner energy sources under the constraints of lower prices and maximum reliability. Although a high penetration level of penetration of wind power mitigates negative environmental impact compared to traditional power plants, control issues are complicated. The conventional power system is synchronous machines based and can help in the frequency control process of the grid due to its high inertia. Unfortunately, wind turbine generators cannot do the same since their rotating mass is separated from the grid via the power electronics converters. This thesis aims to investigate the voltage stability improvement in a rich dominated power system by highlighting the key gaps and cutting edge technologies

including STATCOM, SSSC to handle these issues. Furthermore, ways to augment the reactive power loadabilty of an existing transmission grid by optimally integrating a large wind farm at its weakest bus are studied. This work is harmonized as:

Chapter 1 presents a review of existing background about wind energy worldwide and the problem formulation is introduced. Also, a critical review of the technologies in use to generate power in a wind power system is presented. Some wind power forecasting techniques and the operation of the wind-dominated power system are presented. Furthermore, the modeling of the various components of the system for voltage stability studies is presented. Chapter 2 presents the existing works on the voltage stability of wind power systems. The dynamic voltage stability phenomenon is reviewed with different causes that can trigger them. The classical approaches for the steady-state voltage stability evaluation are presented. Additionally, the voltage stability of the wind power system with type 3 wind turbines is presented. Furthermore, the effects of wind generators' voltage control strategy on voltage stability are presented. The LVRT of DFIG during faulty conditions is presented and accompanied with the cutting-edge technologies to keep the wind farm Online during a Short Circuit. Chapter 4 presents some existing solutions using FACTS for transient-stability amelioration in a wind-dominated power system. Chapter 5 present the results and discussions.
Chapter 6 sums up the conclusions about the work done and presents future work and recommendations.

Chapter 2

Literature Review

This literature survey will present the prior works in the field of wind-dominated power systems and wind turbine technologies. Also, prior works on the modeling of the wind farm for power flow analysis and voltage stability are addressed. Existing forecasting techniques for wind power are also presented.

2.1 Statistics

The integration of wind energy has been growing rapidly worldwide. Between 2003 and 2008, the wind power industry has grown at an average rate of 24%[1]. In 2016, it was reported that wind power installed was 82 143 MW for the USA. By assuming an average market growth, it is easy to forecast that the total capacity worldwide in wind power will be around 1 129 000 MW in 2030 [8]. For instance, only in California and Hawaii, a study revealed that wind generators would generate 20% of the total US demand for electricity by 2030 [7]. Also, these two states have aggressive programs called Renewable Portfolio Standards (RPS) to increase their Renewable penetration levels. A few decades earlier, only the wind penetration levels, worldwide, was low. Presently, the landscape of the power industry is under major changes. 23 other US states have adopted the RPS – goals of producing $15 - 25\%$ of their total generation from wind energy for the period 2020-2025. In that sense, Texas is a fantastic state since they have already met these goals in 2009 when they have integrated into their power grid 8797 MW of wind energy[7].

Modern operate wind turbines can operate with very good efficiency at different wind velocities. The power graph shows the variation of its net power versus the wind speed and has 3 regions namely: cut-in wind speed region, nominal wind speed

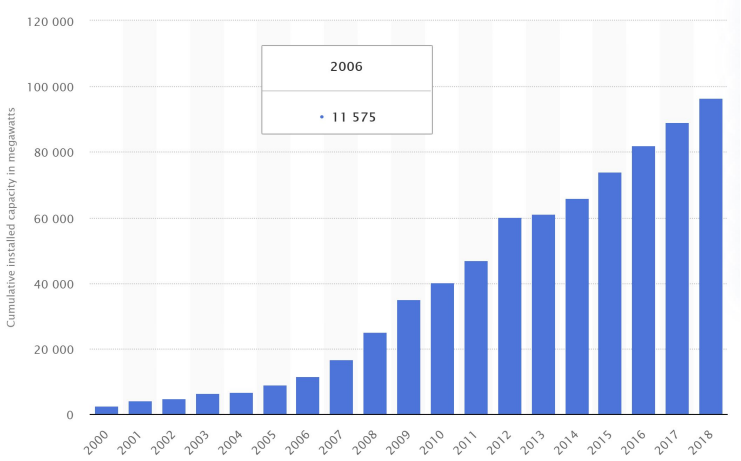

Figure 2.1: US cumulative wind power capacity for 2001-2017 [23]

region, and cut-out wind speed region. The power curve is of the utmost importance in the monitoring of the wind turbine's generator health. In simpler words, it is a tool to predict when maintenance is needed for the wind turbine. By its nature, wind energy is a variable source and so does the power generated. With the blowing of the wind, the mechanical energy is transformed into kinetic energy by the rotor and the gearbox. Wind turbines with larger blades can extract a higher amount of energy. However, the diameter of the wind turbine limits the size of the wind turbine generator. To be able of contributing to the grid significantly, several standard sizes of wind turbines are clustered at a site where there is a good wind profile [43]. The operation of wind turbines causes air turbulence from its back as well as from its sides. The region of turbulence created is termed the wake of the turbine. In the placement of the turbines, none of the turbines are placed in the wake of the forward or side turbines. To be integrated into the transmission grid, each wind farm must meet certain requirements. Voltage sags, faults, and unbalances are very frequent in wind power systems since wind farms exist a great distance from the load center where electrical energy is needed. It is well known that voltage and frequency are two parameters that are of the utmost importance to any grid operator and system planner. In a strong transmission grid, it is easy to reestablish voltage and frequency after a major disturbance. Conversely, it is not so easy in a weak transmission grid.

Waiting for voltage restoration, after the protection systems have cleared the fault, is not secure. Doing so might drive the entire power system into a major blackout. The mitigation of this problem is done by relying on some devices like SVC, STATCOM, and SSSC. The SSSC has the merit to improve the critical clearing time. Also, it can greatly ameliorate the voltage profile of the system. Today's wind power industry is dominated by two types of wind turbines technologies that are: the fixed type and the variable speed generator type. The fixed type wind turbine uses a squirrel-cage induction generation in its operation. A step-up generator connects the generator to the collector of the wind park. Independently to the wind speed, the set generator/rotor speed is maintained constant. The power of the variable speed wind generator is kept constant independently of the wind speed.

The mechanical power power extracted from the wind is computed by:

$$P_m = \frac{1}{2}\rho V^3 \pi r^2 C_p \lambda \tag{2.1}$$

ρ : air density in kg/m^3

V : wind speed in m/s

C_p : performance coefficient

r : radius of the blade (m)

λ : tip speed ratio

The tip speed ratio is given by

$$\lambda = \frac{\omega.r}{V} \tag{2.2}$$

ω denotes the angular velocity of the rotor in radian/second

C_p is derived by aerodynamics laws and is variable from one turbine to another. It represents the power collected by the WT from the available wind. The higher the C_p the higher is the power captured by the WT. Unfortunately, C_p has a value guided by the so-called Betz's law. Also, C_p varies with respect to λ and the blade pitch angle. Fig 1.3 shows the variations of Cp in function of the constant value of λ.

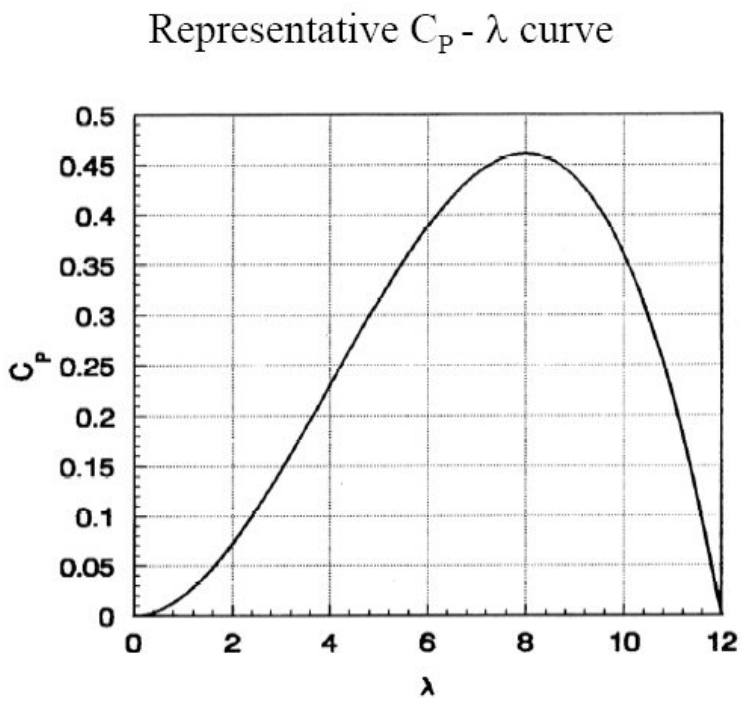

Figure 2.2: The variation of Cp versus tip ratio [13]

Fig 2.2 exhibits the performance coefficient at a given tip-speed ratio. The performance coefficient reaches its highest value at the specific tip-speed ratio and wind speed when C_p is constant. This performance coefficient reaches its maximum value at 0.593 and this value is determined by invoking fluid mechanics constraint termed as the Betz limit. Consequently, Fixed -Speed Wind Turbine is restricted to operate at certain ranges of wind velocity. These issues triggered the need to develop wind turbines that can extract the maximum power possible over a large interval of speeds. These wind Turbines are termed, in the wind power industry, Variable Speed Wind Generators (VSWG). Fig 2.3 presents the variation of Wind Turbine output with angular speed and wind speeds.

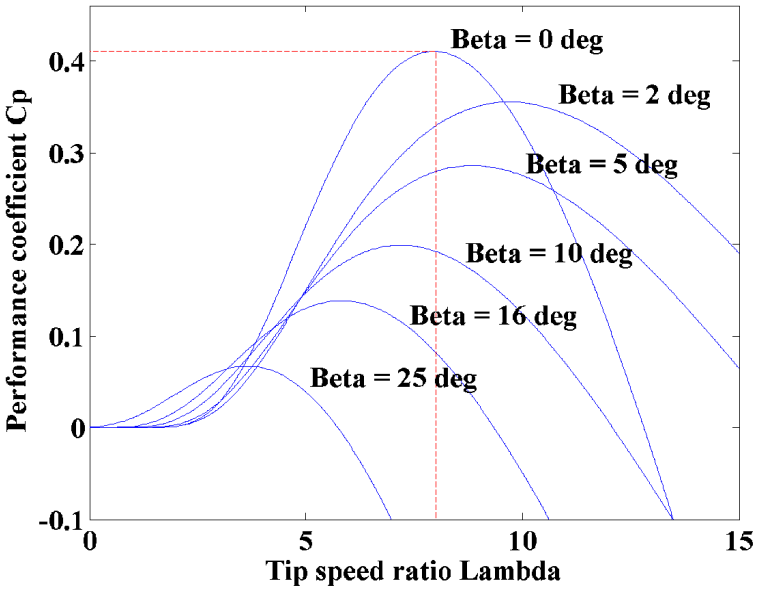

Figure 2.3: Wind turbine output power with respect to speed [14]

2.2 Power Curve of WT

Modern wind turbines can efficiently operate at different wind velocities. A wind turbine's power curve is a graph that shows the variation of its electrical power versus the wind velocity. The power curve has 3 regions namely: cut-in wind speed region, nominal wind speed region, and cut-out wind speed region. Power is of the utmost importance for the wind farm operator to monitor the health of wind turbines generator. This curve is presented in Fig 2.4 with the 3 regions aforementioned.

Electrical power is generated in the wind turbine generator at the cut-in wind speed. Beyond the nominal speed of the wind turbine generator, the wind turbine is shut down for its protection. Furthermore, blade speed pitch is used to mitigate the stress applied on the shaft of the DIFG [32]. Fig 2.5 exhibits a typical diagram of the pitch controller.

The implementation of the wind turbine generator control system is done via a Proportional Integral controller that subtracts the mechanical power from the electrical power. The difference from that subtraction is served as the input signal

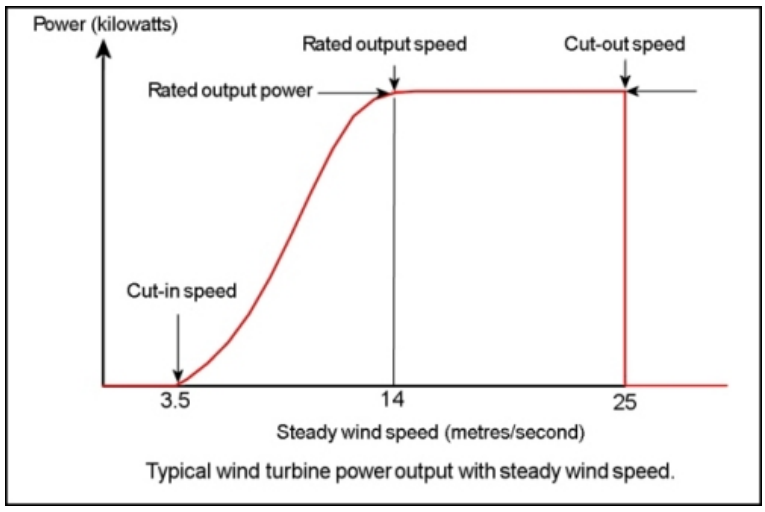

Figure 2.4: Wind Turbine Power Output [10]

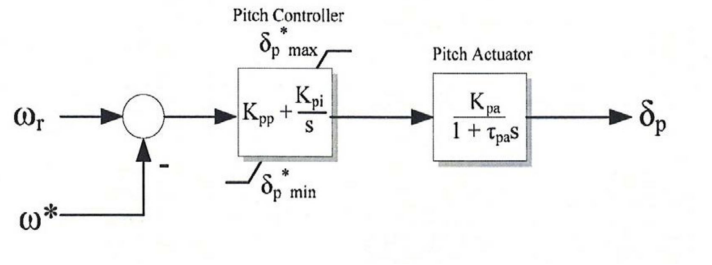

Figure 2.5: Pitch Controller Open Loop Controller [9]

to the pitch controller for control actions. ω^* denotes the reference rotor speed of the generator. A PI controller regulates the position of the blades for optimizing the power extraction at different speeds. If the turbine is operating at a wind speed less than ω^* , the PI controller positions the blades to optimize energy extraction. In high wind velocity periods, the blades are feathered to reduce the power generated by the wind turbine.

2.3 Wind Power Forecasting Techniques

The effective and efficient operation of a wind-dominate power system relies on heavily on accurate wind power output forecasting. Indeed, wind power forecasting is crucial for voltage security assessment, frequency stability, unit commitment, and maintenance scheduling [55]. Several well-established methods are used for wind

power output forecasting. Well-known methods such as sequential Monte Carlo are used alongside time-domain simulations. With no accurate chronological data, it is impossible to use these methods. Furthermore, they are tedious since they consume a lot of time. Wind farm operators use the distribution of the wind speed velocity over a period. For this purpose, the most used probability distribution function is the Weibull distribution. This function presents the probability of the wind velocity for $1m/s$ which has for center a wind velocity value v considering the yearly and seasonal variations. The wind speed probability density function, as stated earlier follows the Weibull distribution. The output power function is a piecewise continuous function as exhibited below.

$$p(v) = \begin{cases} p_1 = P_r - P_r \left[1 + exp(\frac{v - v_{mid}}{c})\right]^{-1} & 0 < v < v_{lim} \\ p_2 = P_r - P_r \alpha (v - v_{mid})^q & v_{lim} < v < v_f \end{cases} \tag{2.3}$$

the parameter v_{mid} is the wind velocity when the speed is 50% of the nominal value. The parameter c must be computed as follow

$$c = (v_r - v_{mid}) \left[\log\left(\frac{\beta}{1-\beta}\right)\right]^{-1} \tag{2.4}$$

P_r denotes the nominal power at the nominal(rated) wind speed V_r . In the realm of the wind power industry, generally , $p_1(v_r) = 0.999 P_r$. The parameter α is computed using the following equation under the constraint $p_2(v_f) = 0$.

$$\alpha = (v_f - v_{lim})^{-q} \tag{2.5}$$

Finally, the wind-speed pdf is distributed as probability versus the output power function. By using the so-called random-variables transformation, the variable v and the pdf $f(v)$ combined with the $p - v$ characteristics for the wind turbine the

following equation can be derived.

$$f_p(p) = \frac{f(v_1)}{\mid p_1'(v_1) \mid} + \frac{f(v_1)}{\mid p_2'(v_1) \mid} \tag{2.6}$$

v_1 and v_2 are obtained by inversing the $p - v$ function as follow.

$$\begin{cases} v_1 = v_{mid} + c.\log\left(\frac{p}{P_r - p}\right) \\ v_2 = v_{lim} + \left(\frac{1}{\alpha}\frac{P_r - p}{P_r}\right)^{\frac{1}{q}} \end{cases} \tag{2.7}$$

The derivation of p_1 and p_2 are

$$\begin{cases} p_1'(v) = \frac{P_r}{c}\exp\left(\frac{v - v_{mid}}{c}\right)\left[1 + \exp\left(\frac{v - v_{mid}}{c}\right)\right]^{-2} \\ p_2'(v) = -2\alpha P_r(v - v_{lim}) \end{cases} \tag{2.8}$$

It is worth noting that the probability output wind power must be recalculated for a certain value of power. Then after,the associated v_1,v_2 is computed followed by the derivative value of p_1, p_2. Finally,the the probability associated to the power is presented [41].

2.4 Unit Commitment Challenges of Wind-Dominated Power Systems

The operation of a transmission grid with an enormous amount of wind energy is a complex task. For instance, maintaining the load balance equation is complicated. The intermittency of wind energy requires a significant need for reserves. Additional reserve means additional operation costs. Peak demand in wind farms occurs in the morning and does not coincide with heavy load conditions. Consequently, if not ancillary services are not called upon, the power system might be frequently unstable. Another challenge is the wind forecasting challenges. Electrical power is generated from the wind farm when the wind is blowing. It is quasi impossible to forecast wind velocity with great accuracy. Consequently, operating a wind-dominated power

system at minimum cost is a complex task for transmission system planners. Indeed, the generation must balance loads all the time. When the wind is not blowing, electric utilities need to call upon conventional power plants to meet the load balance equation. The error in wind power forecast can impact the Unit Commitment of non-wind generation. Under forecasting implies over-commitment of non-wind generation and over forecasting implies Under-commitment of non-wind generation. Both issues are undesirable for the Unit Commitment and Economic Dispatch. Over-commitment can lead to a sub-optimal solution to the ED problem and significantly increase operations cost as well as power curtailment. Conversely, under- commitment can drive the system into voltage collapse and some other reliability problems. To alleviate the issues, it is required to minimize the uncertainty related to wind power during the UC time interval [42].

For all the reasons mentioned above, the UC problem with high wind energy levels is an active area of research [44],[45]. The main objective of the UCP is to determine which unit should be ON/OFF to meet a particular load to minimize the total operating cost [46]. The production levels of the committed units need to be known to satisfy the load balance equation at the lowest cost over the planning horizon. Several constraints affect the minimization of the operating costs which can reduce the search space. To formulate the UC problem, there are many constraints used such as the limits of the generator, the minimum up and down-time requirements, the spinning reserve requirements, minimum up-time/ downtime requirements, the initial status of the unit, and the limits of the ramp rate [47]. The decision variables are the state of units and the output of the committed unit. As a result, the UCP has been viewed as a problem under mixed integers optimization. Energy storage works in tandem with the synchronous generators and Renewable Energy Sources to be charged during the light-load period and discharged at the peak demand period. The combination of Wind Turbine Generators with battery energy storage systems very useful technique to regulate wind power [47],[48]. The Windfarm/thermal UCP

aims to find the best combination between the conventional power plants and the wind farms to minimize the operating cost [48]. The status of the generator is used as the decision variable for the optimization problem[49].

$$C_T = \left[\sum_{t=1}^{T}\sum_{i=1}^{N} C_i\left(P_i^t\right)\right]u_i^t + \left[\sum_{t=1}^{T}\sum_{i=1}^{N} S_i^t\right]u_i^t\left(1-u_i^{t-1}\right) + \left[\sum_{t=1}^{T}\sum_{i=1}^{N} D_i^t\right]u_i^{t-1}\left(1-u_i^t\right)$$

In the equation above, the first component is the total fuel cost which is a piece-wise linear function.

$$C_i(P_i^t) = C_i^{nl} + \sum_{s\in S} FC_{i,s}P_{i,s}^t \tag{2.9}$$

The second component is the start-up cost of the generating units.

$$S_i^t = \begin{cases} S_{hi} & 0 < T_{i,OFF}^t < T_i^D + T_i^C \\ S_{ci} & 0 < T_{i,OFF}^t < T_i^D + T_i^C \end{cases} \tag{2.10}$$

The minimization of the objective objective is subject to the constraints 2.11, 2.12, 2.13 , and 2.14.

$$\left| \quad \right| \qquad PF_{l\,|}^t \leq PF_l^{max} \tag{2.11}$$

The generation limits of all committed units are described by the following equation:

$$P_t^{min} \leq P_i^t \leq P_i^{max} \tag{2.12}$$

The minimum require time a committed or de-committed unit can be switched on is given by the Up and Down periods.

They can be expressed by:

$$\begin{cases} T_{i,ON}^t \geq T_i^U \\ T_{i,OFF}^t \geq T_i^D \end{cases} \tag{2.13}$$

The demand should be met and spinning margin is needed for safety and reliability. The mathematical formulation of this constraint is the following:

$$\sum_{i=1}^{N} P_i^t U_i^t + P_w^t + P_{ESS}^t \geq P_D^t + SR^t \tag{2.14}$$

The summation of total generation of power from thermal units, wind farms, and energy storage system should satisfy the load balance equation.

$$\sum_{i=1}^{N} P_i^t U_i^t + P_w^t + P_{ESS}^t - P_D^t - P_L^t = 0 \tag{2.15}$$

Wind power is a mature technology and is capable to reduce the total production cost of the CO_2 emission level. Unfortunately, wind energy is intermittent by its nature and poses some challenges, especially large-scale wind farms. The randomness of the wind power needs to need to be considered and modeled in the power balance equation constraint. The load balance equation constraint is described by Eq (2.17) and it can be rewritten considering the probability nature of wind resources.

$$Pr\left(\sum_{i=1}^{N} P_i^t U_i^t + P_w^t + P_{ESS}^t \leq P_D^t + P_L^t\right) \leq \sigma \tag{2.16}$$

σ is the power balance tolerance which states when the load balance equation cannot be met. In simpler words, a larger value of σ implies a better usage of the wind energy resources of the wind farm.

$$Pr\left(\sum_{i=1}^{N} P_i^t U_i^t + P_w^t + P_{ESS}^t - P_D^t - P_L^t\right) \geq 1 - \sigma \tag{2.17}$$

The equation 2.18 is the stochastic power balance equation.

2.5 Wind Turbines Technologies

- **Type 1 Wind Turbine Generator**

  These types of WT have limited variables and use a Squirrel-Cage Induction

Generator (SCIG). As defined in [10], they can provide active power to an existent grid. However, there is a challenge of consuming reactive power due to excitation.

- **Type 2 Wind Turbine Generator**

A type 2 wind turbine generator uses a wound induction generator with an external resistor to vary its speed. These wind turbines are inexpensive and do not require a lot of maintenance. However, they have poor voltage control and during a fault, they do not possess any ride-through capability. They can damp the oscillations of the power system to stabilize the grid following a disturbance

- **Type 3 Wind Turbine Generator**

These types of wind turbines are very popular are also called Doubly Fed Induction Generator. They have a very good energy conversion efficiency and provide some ancillary services to the grid. Also, they use a wound induction generator. One of their major drawbacks is the high short circuit contribution during a fault. Moreover, the synchronization to the grid needs to be done cautiously to avoid damages. The rated capacity of this power converter is between $30\% - 50\%$ of the nominal capacity Wind Turbine Generator.

- **Type 4 Wind Turbine Generator**

This wind turbine is categorized under the family of variable speed wind turbines. Also, they have their separate active and reactive power control. Unfortunately, they are expensive because of the components converters.

The picture below shows the four more popular wind turbines used in the world. Typically,worldwide, Types 3 and 4 topology are mostly being sold and integrated.

Table 2.1: Design Choices of Leading Manufacturers of Wind turbine

Name	Share Percent	Model	Power	Rating Diameter	Tip	Speed Power Conversion
Vestas	22.8	V90	3,000 kW	90 m	87 m/s	Asynchronous
GE Energy	16.6	2.5XL	2,500	100 m	86 m/s	PMG converter
Gamesa	15.4	G90	2,000	90 m	90 m/s	DFIG
Enercon	14.0	E82	2,000	82 m	84 m/s	Synchronous
Suzlon	10.5	S88	2,100	88 m	71 m/s	Asynchronous

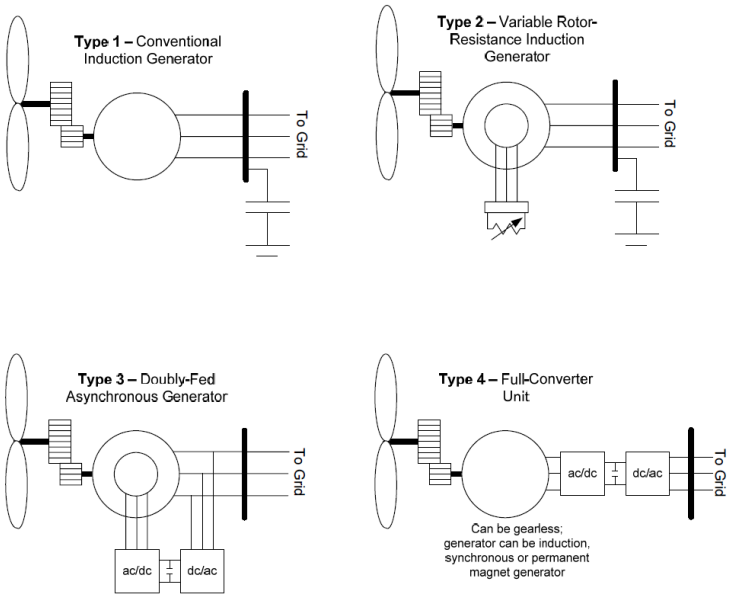

Figure 2.6: Block Diagram of Wind Turbines Type 1,2,3,4 [50]

2.6 Modeling of the Wind Farm for Voltage Stability Studies

Aggregation models of the wind turbines are used to avoid dealing with each turbine individually for voltage stability studies. In doing so, fewer computational resources are needed. The aggregate model should have the same electrical parameters such as power and voltage. It is obvious that wind turbines individually do not affect the power system severely. However, as a collective group, it may harm the operation of a power system during major disturbances [11,[38]. To be valid, the full aggregation

modeling method of variables speed generators need to keep constant wind speeds and mechanical speeds during the specific time interval.

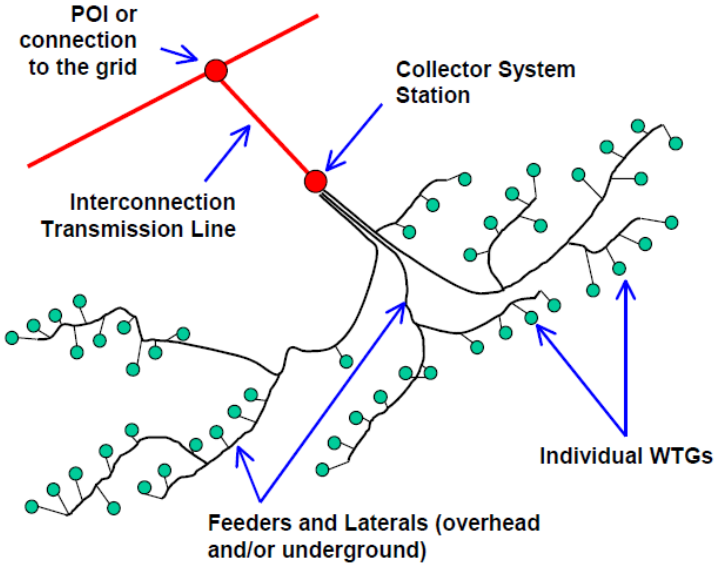

Figure 2.7: aggregate model of a wind [35]

In the power flow studies, for simplicity, the wind farm is reduced to its equivalent since higher numbers of buses would increase the computational time. When reduced to one wind turbine, the equivalent parameters of the machine need to be derived. Let us denote by P_{eq} in MW, Q_{eq} in Mvar respectively the equivalent real power, reactive power of the aggregate model. Furthermore, it assumed that the wind farm has N wind turbines and we can write:

$$\begin{cases} P_{eq} = N.P_{MWperunit} \\ Q_{eq} = N.Q_{MVarperunit} \end{cases} \tag{2.18}$$

N denotes the number of wind turbines generators and the number of pad mounted transformer.

$$\begin{cases} P_{eq} = N.S_{MVAperunit} \\ Z_{eq} = \frac{Z_{perunit}}{N} \end{cases} \tag{2.19}$$

2.7 Load Modeling for Steady-State Voltage Stability Studies

In voltage stability studies, it is not practical to consider each load individually. Generally, the aggregate load model is invoked for dynamic and static studies. Load dynamics impact the voltage stability of the system. The models that are used for the voltage stability studies need to represent as close as possible loads of the power system [62]. The relationship is between load types and voltage is highlighted in the following lines.

- **Voltage dependent loads**

The exponential load model is very popular in power system planning for load modeling. It is represented by

$$P = P_0 \left(\frac{V}{V_0}\right)^{\alpha} \tag{2.20}$$

$$Q = Q_0 \left(\frac{V}{V_0}\right)^{\beta} \tag{2.21}$$

P_0 , Q_0 and V_0 are respectively initial active power, reactive power, and voltage and α and β are loads exponents. The most widely used loads models are constant power loads, constant current loads, and constant impedance loads. For Constant power loads $\alpha = \beta = 0$, for constant current loads $\alpha = \beta = 1$,and for constant impedance loads $\alpha = \beta = 2$.

- **Polynomial Load Model**

Polynomial loads models are used in the design and planning of power system since they give a more accurate representation of power system loads [15]. A polynomial load model is represented in the following form:

$$P = P_0 \left[a_1 \left(\frac{V}{V_0}\right)^{\alpha_1} + b_1 \left(\frac{V}{V_0}\right)^{\beta_1} + c_1 \left(\frac{V}{V_0}\right)^{\gamma_1} \right] \tag{2.22}$$

$$Q = Q_0 \left[a_1 \left(\frac{V}{V_0} \right)^{\alpha_2} + b_1 \left(\frac{V}{V_0} \right)^{\beta_2} + c_1 \left(\frac{V}{V_0} \right)^{\gamma_2} \right] \tag{2.23}$$

where: $a_1 + b_1 + c_1 = 1$

ZIP which is, constant power, constant current, constant impedance, is the most common type of polynomial load.

2.8 Control Scheme of Wind Farm during Faults Conditions

DIFG wind turbines generators are extremely popular in the wind power industry and have three primary controllers. Two of the controllers are used for voltage, frequency per active power of the wind generator. Also, the other controller is used to regulate the pitch angle. I n this work, the control for the wind turbines comprises two parts namely: basic control strategy for steady-state operation, specified control for grid faults, and grid codes obligation to meet. The control strategy is incorporated to optimally capture the energy of the wind turbine. Another control included is the fault ride-through which is essential in keeping the wind turbine online during the faulty condition [29],[34].

Synchronous generators are among the major components of a traditional power system. Because of their high inertia, synchronous generators react very well to most of the major system disturbances. The behavior of disturbances, on the grid, towards synchronous generators is richly documented in the literature of power systems. Wind turbines do not possess high inertia compared to a traditional synchronous generator. Consequently, they react differently with the transmission grid when they are subjected to faulty conditions on the traditional power systems [33],[39]. The terminal voltage amid fault can be found by using the equivalent network model. The voltage at the PCC is found by using the voltage divider model presented in Fig 2-8 for a fault from the external grid.

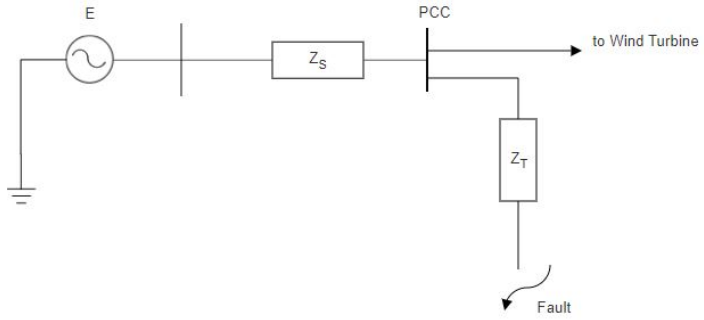

Figure 2.8: Three-phase fault illustration at the PCC

The voltage at the PCC amid faulty condition is given by:

$$V_{PCC} = \frac{E.Z_T}{Z_T + Z_s} \tag{2.24}$$

Amid the fault period, the voltage at the PCC is considerably reduced to a certain interval. The Low Voltage Ride Trough capability is the ability of wind turbines to operate uninterruptedly while keeping their connection to the AC transmission grid [6]. LVRT assists to balance the system and maintain frequency amid and after major disturbances. Thus, Wind turbines without LVRT capability may trip during faulty conditions [4]. The (FERC) Order No.661 stipulates that the wind farm should stay online for a voltage 15% for 0.625 seconds. Also, for the High Voltage side, the wind farm should stay online for voltage around 90% of the nominal line voltage [16].

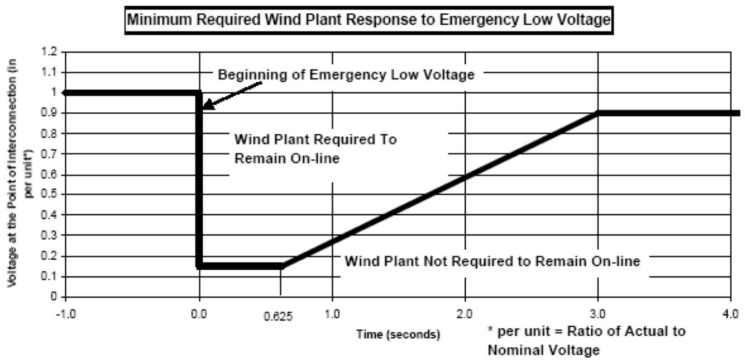

Figure 2.9: Fault Voltage Ride Trough by FERC [16]

Unlike synchronous machines, the power of the wind farm is variable. As such,

voltage variations are induced from these power variations resulting in ramifications for the power systems and consumer. Furthermore, the deployment of these power electronics-based converters increases the harmonics content of the voltage and current generated. Considering the deployment of these wind farms and the strength of the existing transmission grid, developing a suitable control strategy to keep them Online during fault conditions is an obligation.

2.9 Frequency Control Capability

For grid operators, frequency is among the extremely important parameters to monitor. As the grid is witnessed a huge deployment of large wind farms, grid operators are implementing several rules for frequency requirements. Wind farms need to behave like the traditional power plant in terms of frequency requirements. The frequency should remain inside a band. For example, the ERCOT's operating guide has the following requirements for under and over-frequency requirements.

Table 2.2: ERCOT's operating guides for Under-frequency and Over-frequency
Requirements

Range of Frequency	**Trip Delay**
$f < 59.4$ Hz	None(operating continually)
$58.4 \leq f \leq 59.4$	Greater than or equal 9 min
$58.0 \leq f \leq 58.4$ Hz	Greater than or equal to 30 sec.
$57.5 \leq f \leq 58.0$ Hz	Greater than or equal to 2 sec.
$f \leq 59.4$ Hz	No delay

Frequency deviation from the limits above has detrimental impacts on the wind power plants and might lead to systems blackout. Most the, the transmission system need to schedule traditional power plants to provide ancillary services to restore the frequency of the system. This Remedial action might augment the operating cost of the power system.

Chapter 3

Steady-State Voltage Stability Assessment

The buses voltage of the power system should stay inside a prescribed interval during normal operation. However, if subjected to major disturbances, the buses voltage of the power system might deviate from the permissible ranges. A power system that is voltage stable can easily bring back the power system to a new equilibrium point to avoid voltage instability. Indeed, a power system is voltage stable if and only if it is capable of maintaining the voltage levels at each bus during normal operation or after a major disturbance inside the permissible interval [18],[19]. If not well-properly, this dynamic phenomenon may result in various detrimental economic, technical effects. Following several contingencies and voltage collapse worldwide, researchers and scholars are busy trying to study, understand and derive ways to mitigate voltage instability. Voltage collapse is a continuous reduction of the voltage magnitude levels [18]. In the beginning, the voltage starts to decrease gradually and after to decrease more rapidly and drive the power system into instability.

Many factors can contribute to voltage instability in a power such as [15]. • High loading of the power system

•Inadequate reactive power

•Load characteristics at low voltage

•Under voltage Load Changers responding to low voltage at load buses •Mal-operation of relay amid low voltage magnitudes

Voltage instability is a dynamic phenomenon; as a result, the transient simulation might be used during voltage stability studies. Unfortunately, this kind of simulation is not suitable for sensitivity analysis and stability level indication. Furthermore, these simulations require a long computational time and are tedious for the analysis of the results. Thus, the so-called steady-state analysis approach is more appropriate and furnishes information about the reactive power loads problems [17],[13]. Keeping a healthy voltage profile at a particular bus does not imply voltage stability. Other causes rather than low voltages might be the causes of the voltage instability. Also, the modeling of the On-Load Tap Changers, Over- excitation limiters, are required during dynamic simulations [19],[22]. Several standards are used to classify the voltage stability problem such as the nature of the disturbances to which the power grid has been subjected. Also, the time scale is very important is considered for this classification. As a result, this problem is classified into short-term voltage stability and long-term voltage stability. As the power system is one of the most complicated man-made systems, and is always continually in a dynamic state and never in a pure steady-state mode. This observation leads to the division of the voltage stability problem into the categories presented in Fig 3.1.

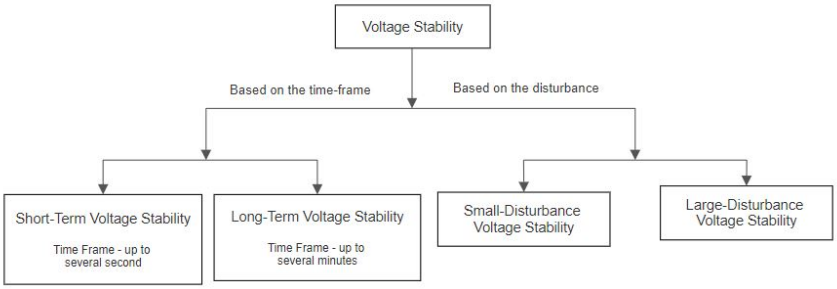

Figure 3.1: Classification of voltage stability

The voltage stability phenomenon is slow, and the voltage magnitudes of the system might witness a large voltage drop in a noticeably short time following a disturbance [16]. Several experts in voltage stability have classified the voltage instability and collapse according to different time frames [18],[19]. These two categories are the following:

- Short-term voltage instability: The span is up to several seconds and is initiated by the behavior of dynamic loads like induction motors followed by a major disturbance.

- Long-term voltage instability: This has been recently introduced to the power system area. This phenomenon can last more than several minutes and is initiated by major disturbance and /or sudden load change or augmentation in power transfer [18],[19].

- Large -disturbance voltage stability: It mainly refers to the capability of the grid to keep the voltage magnitudes of each bus inside the permissible ranges after system faults, loss of one or more transmission lines, or loss of important generating units [18]. To capture this phenomenon, the non-linearity dynamic performance of the power grid should be examined over a reasonable time interval to assess the impact of ULTCs and the field currents limiters of the generators [18],[19]. I t is current practice to consider a time interval of a few

seconds to tens minutes to study this phenomenon using long-term dynamic simulations.

- Small -disturbance voltage stability: It is mainly related to the capability of the

grid to keep the bus voltage within the permissible ranges for small disturbances such as small load increase [18],[19].

3.1 Methods of Steady- State Voltage Stability Analysis

The power flow or the load flow is a bread and butter for any power systems operations engineer, and power system design engineer. It solves the steady-state power equations of the network. Power flow is a prerequisite for economic operations studies, stability studies, contingencies analysis. The information obtained is the voltage levels, the voltage angle, real and reactive power, and line flows. Adding new generation, load, or transmission lines to an existing power system has several impacts. In this work, the power flow is done using DigSilent, ETAP, and PSAT/Simulink.

3.1.1 The Newton- Raphson (NR) Method

The power flow gives to the power system planners, operators, designers the four vital parameters in a power system namely: real power and reactive power injected, voltage magnitude, and the angle at a particular bus. The Newton-Raphson is a popular method to solve the power flow problem since it converges faster. As the load flow is a non-linear problem, an iterative approach is required to approximate the solution. The time required to approximate the solution augments linearly with the size of the system [14]. Let us assume that

we have n non-linear equations as follows:

$$\begin{aligned} f_1(x_1, x_2..., x_n) &= b_1 \\ f_2(x_1, x_2..., x_n) &= b_2 \\ &\cdots \\ f_n(x_1, x_2..., x_n) &= b_n \end{aligned} \tag{3.1}$$

The exact solution vector is not known and we must have some initial guess to start the iteration process.

let us have: $x_0^1, x_0^2, x_0^3, ...x_0^n$ as the guess vector. The correction factors are : $\Delta x_1, \Delta x_2, \Delta x_3, ..., \Delta x_n$.

These correction factors are added to initial solutions so that the equations are met. Thus, we can write :

$$\begin{aligned} f_1(x_1^0 + \Delta x_1, x_2^0 + \Delta x_2..., x_n^0 + \Delta x_n) &= b_1 \\ f_2(x_1^0 + \Delta x_1, x_2^0 + \Delta x_2..., x_n^0 + \Delta x_n) &= b_2 \\ &\cdots \\ f_n(x_1^0 + \Delta x_1, x_2^0 + \Delta x_2..., x_n^0 + \Delta x_n) &= b_n \end{aligned} \tag{3.2}$$

The Taylor series expansion can be used for any of the n non-linear equations. The Taylor series expansion applied to the i^{th} equation gives;

$$f_n(x_1^0+\Delta x_1, x_2^0+\Delta x_2..., x_n^0+\Delta x_n) = f_i(x_1^0, x_2^0..., x_n^0)+\left(\frac{\delta f_i}{\delta x_1}\right)_0 \Delta x_1+...+\left(\frac{\delta f_i}{\delta x_n}\right)_0 \Delta x_n \tag{3.3}$$

Higher-order terms are neglected to simplify life and the the updated solution is calculated by using the following relationship:$x_i^1 = x_i^0 + \Delta x_i$

3.1.2 Power Flow Solution Through N-R Method

Researches conducted in voltage stability widely used power flow analysis as a computational tool. The current injection at each node is :

$$I = Y_{Bus}.V = \frac{S^*}{V^*} \tag{3.4}$$

I = current injection matrix at each node

V= nodal voltage vector

S= nodal apparent power

Y= system nodal admittance matrix

The NR method relies on repetitive linearization of the expansion of the non-linear equation

$$I_k = \sum_{m=1}^{n} Y_{km}.V_m, \forall k = 1, 2, 3...n \tag{3.5}$$

n = number of the bus.

$$P_k - jQ_k = V_k^*.I_k = V_k^* \sum_{m=1}^{n} Y_{km}.V_m \tag{3.6}$$

By using the following polar forms representation: $V_k =\mid V_k \mid e^{j\theta_k}$,$\mathrm{V}_m =\mid V_m \mid e^{j\theta_m}$ $Y_{km} =\mid Y_{km} \mid e^{j\gamma_{km}}$

$$\mathrm{P}_k + jQ_k = \sum_{m=1}^{n} Y_{km}.V_m V_k \cos(\theta_k - \theta_m - \gamma_{km}) + j \sum_{m=1}^{n} Y_{km}.V_m V_k \sin(\theta_k - \theta_m - \gamma_{km}) \tag{3.7}$$

The power imbalance at bus k is: $\Delta P_k = P_k^{sch} - P_k, \Delta Q_k^{sch} = Q_k^{sch} - Q_k$

To solve the non-linear equation, the portioned matrix below is used.

$$J \begin{bmatrix} \Delta\theta \\ \Delta V \end{bmatrix} = \begin{bmatrix} \Delta P \\ \Delta Q \end{bmatrix} \tag{3.8}$$

ΔP: imbalance active power vector

ΔQ : imbalance reactive power vector

ΔV: unknown voltage magnitude

$\Delta\theta$: angle correction vectors

J : Jacobian matrix of the system

The Jacobian matrix is derived by using the apparent power equation and we have:

$$J = \begin{bmatrix} \frac{\partial P_k}{\partial \theta} & \frac{\partial P_k}{\partial V} \\ \frac{\partial Q_k}{\partial \theta} & \frac{\partial Q_k}{\partial V} \end{bmatrix}$$

Reactive power can be decoupled to phase angles since reactive power is correlated to voltage magnitude. Similarly, real power variation is insensitive to voltage magnitudes but most sensitive to variation in phase angle. As a result, the Jacobian matrix can be written as:

$$J = \begin{bmatrix} \frac{\partial P_k}{\partial \theta} & 0 \\ 0 & \frac{\partial Q_k}{\partial V} \end{bmatrix} \tag{3.9}$$

After solving the Eq 3.8,the updated value can be found using the following formula:

$$x(i+1) = \begin{bmatrix} \theta(i+1) \\ V(i+1) \end{bmatrix} = \begin{bmatrix} \theta(i) \\ V(i) \end{bmatrix} + \begin{bmatrix} \Delta\theta(i) \\ \Delta V(i) \end{bmatrix} \tag{3.10}$$

The stop criteria for the iteration process are based on the power mismatches instead of the voltage magnitude mismatches. Because of its quadratic convergence, the NR

method converges after a few iterations. However, a poor starting solution and a lack of reactive power support can lead to convergence problems.

3.2 Steady-State Voltage Stability Assessment Trough QV Curves- QV Curves Inter-stability margin

Voltage stability is seen as a steady-state problem and power flow remains the most used method to study this phenomenon. Voltage stability can be viewed differently by power system engineers since it encompasses a broad range of phenomena [18]. The steady-state loadability limits of the power system are analyzed by using P-V and QV curves. The QV relation exhibits the variation of the bus voltage versus reactive power injections or absorption [18]. In the region where the QV sensitivity is positive, the system is voltage stable. Otherwise, the system is voltage unstable and cannot meet its reactive power demand [20]. Furthermore, electric utilities around the world use these curves to assess how far a power system is from unstable mode. Also, transmission systems operators use these curves to verify if the voltage of the system can be maintained for a particular loading condition. The disadvantages of Q-V curves are it is almost impossible to know in advance at which bus to generate the Q-V curve. To address these issues transmission system operators, use voltage level at each bus as an index of voltage instability.

3.2.1 QV Curves

The QV curves are among the classical methods that electric utilities use to evaluate voltage stability. This mainly shows the sensitivity of the bus voltage for the reactive power injected. This curve can tell the grid operator how much reactive power the weakest bus can handle before the voltage collapse of the system [20]. With these curves, the grid operators can have an intuition about the Remedial Action

Schemes to take to keep the system stable. To plot the QV curves, traditionally, an imaginary generator is attached to the test bus while the reactive power of the bus is being recorded [20]. The MAVAR value of the generator will reach a point where its output stops to decrease. This point is the maximum increase in load that can occur at this bus before the voltage of the system collapse [18],[19]. Fig 3.2 represents a typical QV plotted for a bus bar.

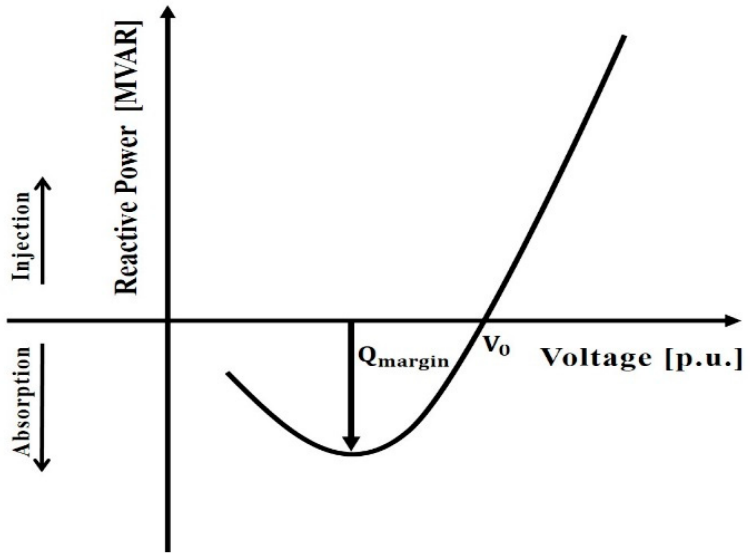

Figure 3.2: Typical QV Curve

The Q_{margin} tells the grid operator the closeness of the system to voltage instability. In simpler words, it is a warning point to the grid operator. The y axis exhibits the reactive power to be added or removed to the bus under investigation to keep the voltage between the permissible range. Around the minimum point of curve of the Q-V curve, sensitivities get large with a notable change. For the same value of power, the curve has two values for the voltage. To keep the power constant, the power system in operation with the lower voltage will need a high current to satisfy the power demand. For this reason, the minimum of the Q-V curve is termed an unstable region and beyond this point, the voltage of the system will collapse. The grid operator should avoid this point.

Around a solution, the non-linear equation system can be linearized and we can write

the following equations.

$$J \begin{bmatrix} \Delta\theta \\ \Delta V \end{bmatrix} = \begin{bmatrix} \Delta P \\ \Delta Q \end{bmatrix} \tag{3.11}$$

The J matrix is termed the Jacobian matrix and its elements show the information about the correlation between a small variation of voltage angle and the voltage itself at a particular bus. During the plot of the QV curves, the real power of the system is maintained constant while the steady-state voltage stability being carried out considering the gradual change relationship between Q and V. Since $\Delta P = 0$ we can write:

$$\Delta Q = J_R \Delta V \tag{3.12}$$

where : $\mathrm{J}_R = \left[J_{QV} - J_{Q\theta} J_{P\theta}^{-1} J_{PV} \right]$

This equation can be rearranged as:

$$\Delta V = J_R^{-1} \Delta Q \tag{3.13}$$

$J^{-1}{}_R$ denotes the reduced Jacobian Matrix. The i^{th} diagonal elements of this matrix are the $Q - V$ sensitivity at bus i with $i \in [\![1, n]\!]$. n is the set of buses of the power system under investigation. Due to its efficiency, power system planning engineers use the aforementioned equations to compute Q-V sensitivities.

3.2.2 PV Curves

PV curves are another tool used by transmission system operators to evaluate voltage security. These curves, also called the power-voltage curve, tell the grid operator how much MW that can be added to the system before reaching the critical voltage. The

plot of this curve is done by augmenting gradually the real power of the load at the bus under investigation while its voltage is being recorded [18]. Fig 3.3 presents an example of a PV curve. Above to the operating point O', while the real power at the bus is augmenting, the voltage diminishes. The point O' is termed as the unstable region of the system and is the highest power the system can transfer before reaching instability. Beyond point O', the power flow does not converge. A novel method called the continuation power flow has been developed to show the new operating point beyond the critical point [23]. This method is used to determine the operating points beyond the critical point [23].

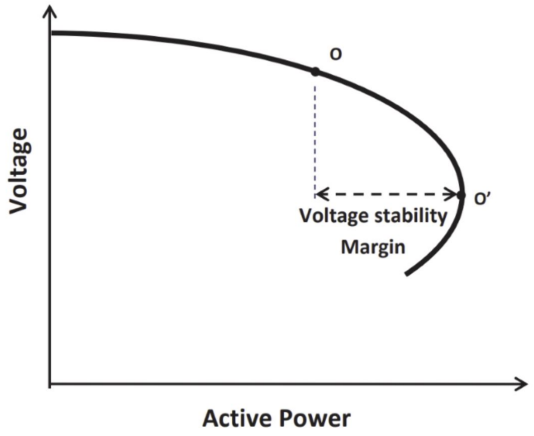

Figure 3.3: Typical PV Curve

3.2.3 Steady-State Voltage Stability Assessment Using Modal Analysis

The modal analysis relies heavily on the Jacobian matrix to predict voltage instability [25]. From the N-R Power-flow we can write:

$$\begin{bmatrix} \Delta P \\ \Delta Q \end{bmatrix} = \begin{bmatrix} J_{11} & J_{12} \\ J_{21} & J_{22} \end{bmatrix} \begin{bmatrix} \Delta\theta \\ \Delta V \end{bmatrix} \tag{3.14}$$

The voltage stability is mainly related to its ability to meet its reactive power demand thus, $\Delta P = 0$ and the following relations are derived:

$$0 = -J_{11}\Delta\theta + J_{12}\Delta V,$$
$$\Delta\theta = -J_{11}^{-1}J_{12}\Delta V,$$
$$\Delta Q = J_{21}\Delta\theta + J_{22}\Delta V,$$
$$\Delta Q = J_R\Delta V$$

J_R is the reduced Jacobian and is given by:

$$J_R = \left[J_{22} - J_{21}J_{11}^{-1}J_{12}\right]$$

By solving for ΔV we have:

$$\Delta V = J_R^{-1}\Delta Q$$

This method relies on the computation of the eigenvalue and the eigenvectors of the reduced Jacobian matrix to predict the voltage stability. Based on the magnitudes of these eigenvalues, one can depict the closeness to voltage instability. Also, the eigenvectors exhibit how the system loses voltage stability.

$$J_R = \Phi\Lambda^{-1}\Gamma$$

Φ = right eigenvector matrix of J_R

Λ = left eigenvalue matrix of J_R

Γ = diagonal eigenvalue matrix ofJ_R

By replacing J_R^{-1} in the QV sensitivity equation we have:

$$\Delta V = \sum_{i=1}^{n} \frac{\Phi_i \Gamma_i}{\lambda_i} \Delta Q \tag{3.15}$$

Eq 3.15 presents the response of the system concerning each mode and the bus of the system with the highest participation factor for the lowest is very fragile in terms of voltage stability.

λ_i and Φ_i and are eigenvalues and the right eigenvalue of reduced Jacobian and Γ_i defines the i^{th} mode of the power system. The i^{th} modal reactive power variation is defined as:

$$\Delta Q_{mi} = K_i \Phi_i$$

where K_i is a scale factor to normalize vector ΔQ_i so that

$$K_i^2 \sum_{j=1}^{n} \Phi_{ji}^2 = 1$$

The associated i^{th} modal voltage variation is:

$$\Delta V_{mi} = \frac{1}{\lambda_i} \Delta Q_{mi}.$$

This equation shows the system is stable λ_i for positive otherwise the system is unstable. If λ_i is zero, the system is going into voltage instability. Additionally, for voltage stability characteristics analysis, small eigenvalues of J_R tells the proximity of the system to voltage instability [24]. The bus participation factor indicates the bus which has a deficit of reactive power system. Generally, buses with high part participation factors are weak or heavily loaded. Also, the participation factor might be useful for reactive power compensation.

3.2.4 Steady-State Voltage Stability Assessment Using P-Q Curves

Voltage collapse in a power system when the total loads of the increases above a certain value. In the assessment of the voltage stability using P-Q regions, the focus

is not only the analysis of the PV buses but also the PQ buses. In the integration of a new wind farm into an existing transmission system, the transmission engineer, the design system engineers, the transmission system operators need to consider the strength of the system to which the wind farm will be connected. Failure to do so might drive the system into voltage instability or voltage collapse. The maximum loadability of a power system is assessed via PV and QV curves. The power flow does not converge beyond the nose curve point and the voltage of the power system will decrease uncontrollably. However, the load characteristics of the power system need to be considered while evaluating the maximum loadabilty of the power system. The P-Q method is a composite of the PV and QV methods. It considers a set of power flow cases while considering the variation of P and Q. By denoting P_{CR} and Q_{CR}, the voltage stability limits using the P-Q method can be computed as follows:

$$S_L = P_{CR} + jQ_{CR} \tag{3.16}$$

This power is the maximum laodabilty of the system and any load value greater than this apparent power will drive the system into instability. To connect a wind farm into an existing transmission grid, the main driver is, generally, the wind pattern of the area. So, it is vital to decide the optimal placement of the wind farm.

3.3 Reactive Power Requirements in a Power System

Most of the newly erected wind farms use DIFGs to generate electrical power [26]. The wind turbine generators are different from the traditional synchronous generators. Also, the variable nature of wind energy makes it more complicated for a transmission system operator to meet the reactive power demand. Accurate models of the DFIG units are crucial for the static and dynamic analysis performance of a given power system [18],[26]. Reactive power flow to the loads from the generator is important to keep the bus voltage within the tolerable ranges [26],[27],[28]. Static and dynamic

reactive power sources are critical for maintaining voltage stability in a power system. DFIG units must have reactive support capability during faulty conditions according to certain requirements. FERC orders 661 and 661 A, released in 20005, established the interconnection requirements for wind farms more than 20 MW [16]. As stated in this order, for the operation of a plant, the power factor at the PCC should be inside 0.95 leading and 0.95 lagging. The reasons behind this ruling are the reactive capability of a wind farm is more costly compared to traditional synchronous generators which have inherent reactive power capability. Imposing these power factors limitations in the operations of a wind farm significantly increases the operating cost

3.3.1 Control System of Doubly Fed Induction Wind Turbine

This control strategy aims to control the voltage and the frequency of the DFIG. This control system has two part which is connected via a DC-link capacitor. The rotor speed and frequency are tracked and regulated by the Rotor Side Converter. The power circulates from the DC-link to the grid if and only if the DC link voltage becomes too high. Otherwise, the power moves from the grid to the DC-link [43]. This control system is implemented by using a back-to-back converter.

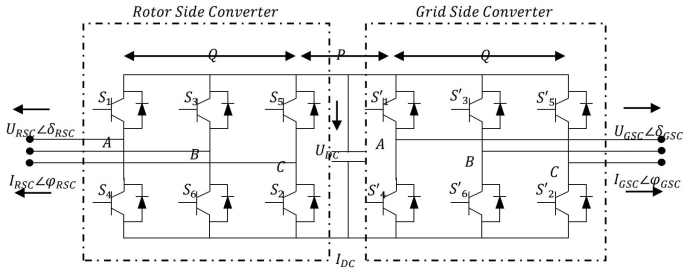

Figure 3.4: Back-to-Back converter typical model

The self-commutated converter above operates at a very high frequency to reduce the harmonics contents of the signal. The switching frequency is often 3kHz. These converters are made of IGBTs which are capable of handling 690V and 400 A

To model the induction machine of the DFIG of the WT, park's transformation is used and we have the following equations:

The stator and rotor voltages are:

$$\begin{cases} V_{sd} = R_s i_{sd} + \dfrac{d\phi_{sd}}{dt} - \omega_s \phi_{sq} \\ V_{sq} = R_s i_{sq} + \dfrac{d\phi_{sq}}{dt} - \omega_s \phi_{sd} \\ V_{rd} = R_r i_{rd} + \dfrac{d\phi_{rd}}{dt} - (\omega_s - \omega)\phi_{rq} \\ V_{rq} = R_r i_{rq} + \dfrac{d\phi_{rq}}{dt} - (\omega_s - \omega)\phi_{sq} \end{cases} \tag{3.17}$$

Stator and rotor fluxes:

$$\begin{cases} \phi_{sd} = L_s i_{sd} + M i_{rd} \\ \phi_{sq} = L_s i_{sq} + M i_{rq} \\ \phi_{rd} = L_r i_{rd} + M i_{sd} \\ \phi_{rq} = L_r i_{rq} + M i_{sq} \end{cases} \tag{3.18}$$

3.4 Control System Scheme of Rotor Grid Side Converter of DFIGs

As the GSC, the RSC is a controllable voltage source and is implemented in the reference dq. The internal current control loops control the stator current components i_{ds} and i_{qs} which facilitates the control of the real and reactive power of the wind turbine generator[[43]. The rotor speed and the reactive power are regulated by the outer loops. These control schemes are implemented via PI control mode. The input to the PWM of the converter is the signalsv_{ds} $\_ref$ and v_{qs}_ref.

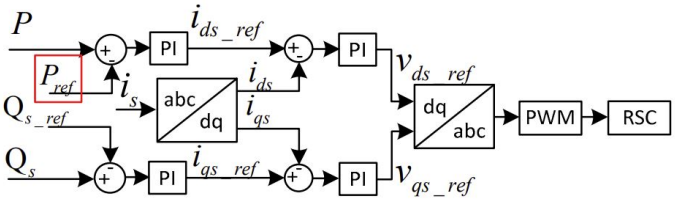

Figure 3.5: RSC control system [43]

3.5 Control System Scheme of Grid Side Converter of DFIGs

The grid side converter control system comprises two control loops. The main purpose of the GSC is to regulate the voltage of the capacitor. Also, the GSC regulates the $d-axis$ current and the $q-axis$ current. The reactive power of the grid side converter is controlled by q-axis current i_{qr}. The input signal to the PWM is the output voltage v_dr-ref. A standard GSC control system block is presented in Fig 3.6

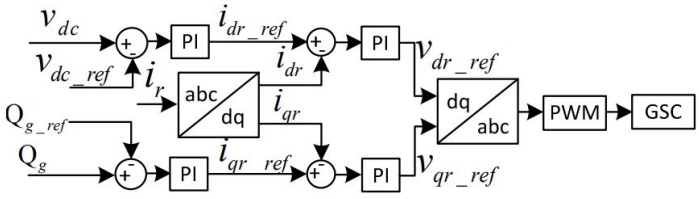

Figure 3.6: GSC control system [43]

Power can be fed into the grid by the DIFG based on its speed. In super-synchronous power is injected into the grid. However, in sub-synchronous mode, the DFIG draws power from the grid.

3.6 Wind Turbine Generator Capacity Curve (WTG)

The reactive power limitations of the traditional synchronous generators are imposed by the insulation and the cooling system of the machine. The alternator is designed to carry a specific amount of current and beyond that current, its coils might be irreversibly damaged. Therefore, the reactive power support of the traditional

synchronous machines is limited. The doubly-fed induction, in opposition to the single-fed induction generator, can operate at different wind velocities. The figure below shows the relationship of the power versus various wind speeds for the DFIG.

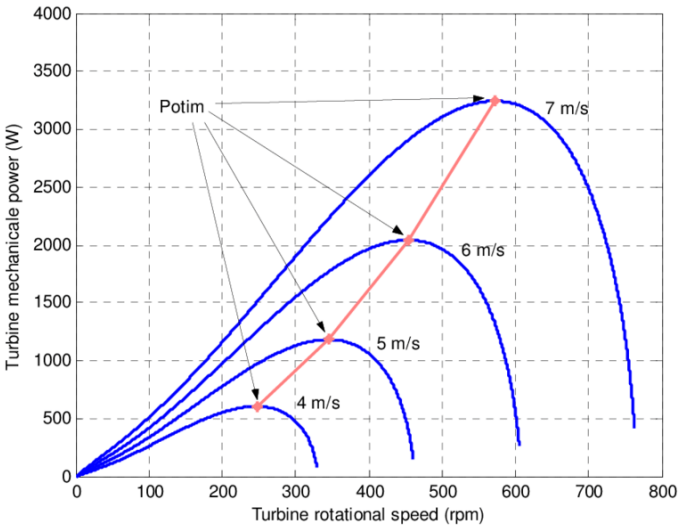

Figure 3.7: Maximum Power Tracking Scheme DFIG [43]

The voltage of the stator of the wind turbine generator is dictated by the voltage of the transmission grid. Furthermore, the rotor voltage and current are imposed by the converter design while the stator is imposed by the generator design.

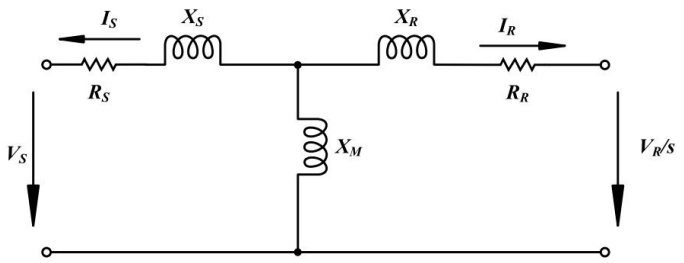

Figure 3.8: Equivalent circuit of a doubly fed induction generator

According to Fig 3.5, the following equations can be derived for the power of the wind turbine generator.

$$P_s = 3\frac{EV_s}{X_s}\sin\delta \tag{3.19}$$

$$Q_s = 3\frac{EV_s}{X_s}\cos\delta - 3\frac{V_s^2}{X_S} \tag{3.20}$$

Also, for the active and reactive power of the rotor these equations can be derived.

$$P_R = -3s\frac{EV_s}{X_s}\sin\delta \tag{3.21}$$

$$Q_R = -s\left(3X_R I_R^2 + 3\frac{EV_s}{X_s}\cos\delta - 3\frac{V_s^2}{X_S}\right) \tag{3.22}$$

The stator active and the rotor active are coupled by the slip s using the following relationship:

$$\begin{cases} P_R = -sP_S \\ s = \frac{\omega_s - \omega_r}{\omega_s} \end{cases} \tag{3.23}$$

From Eq 3.21, the rotor active power of the DFIG unit is negative during the super-synchronous mode of operation. However, the rotor active power is negative when the slip$s$ is positive.

The total active of the DIFG unit is given by.

$$\begin{cases} P_T = P_s + P_R \\ P_T = (1-s)P_s \end{cases} \tag{3.24}$$

The total reactive power of the DFIG unit cannot be found by the summation of reactive power of the rotor and the stator since reactive does not flow from the rotor to the DC link. During the computation of the total reactive power of the DFIG, $Q_{W,g}$, the reactive power reference for the Grid Side Converter, is set to zero. The total reactive power of the DFIG is computed as follows.

$$Q_T = Q_s + Q_{GSC} \tag{3.25}$$

The power capability of a Wind Turbine Generator type 3 for the GSC and the RSC is presented in Figs 3.6 and 3.7.

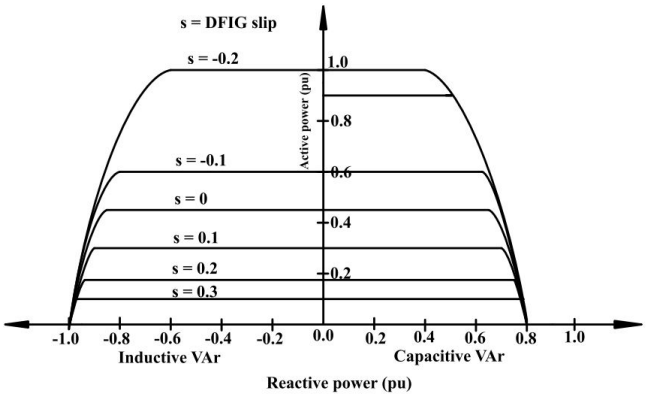

Figure 3.9: DFIG-RSC capability

From Fig 3.7, the rotor side grid converter of a type 3 wind turbine generator can generate power with a power factor pf such that $pf \in [-0.95, 0.95]$. Based on this variation, one can justify the need for reactive power compensation.

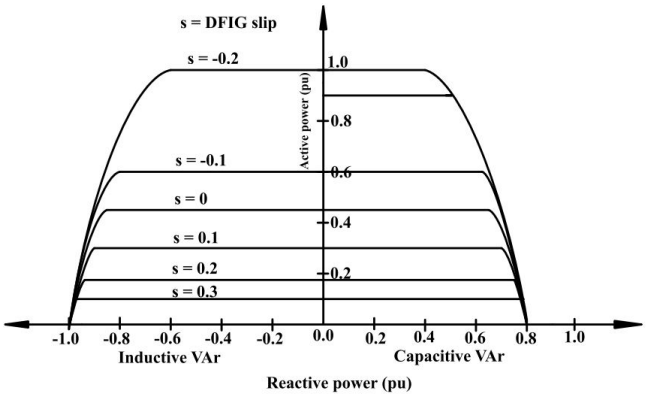

Figure 3.10: DFIG-RSC capability

The derivation of the reactive power limit of the DFIG and the nominal current of the stator need to be performed. Also, the power capability of the GSC needs to be included

$$\overline{V_s} = V_s \angle 0$$

$$\overline{I_s} = I_{s,real} + jI_{s,imag} \tag{3.26}$$

To compute the reactive limit for the nominal current of the stator at a given speed v, $I_{s,real}$ can be calculated as follow:

$$I_{s,imag} = \pm\sqrt{I_{s,rated}^2 - I_{s,real}^2} \tag{3.27}$$

Where $I_{s,rated}$ is the nominal current of the stator and the rotor. The rotor current can be computed as follow:

$$\overline{I_r} = \overline{I_s} - \overline{I_m} \tag{3.28}$$

The complex power of the stator can be computed as:

$$S_s = -\overline{V_s {I_s}^*} = P_s + jQ_s \tag{3.29}$$

The total real power is

$$P_{tot} = P_s + P_r \tag{3.30}$$

The reactive power capability of the GSC is

$$Q_{GSC} = \pm\sqrt{{S_{GSC}}^2 - {P_r}^2} \tag{3.31}$$

Q_{GSC} is the rated capacity of the converter.

3.6.1 Steady-State Model of DFIG

Accurate models of the DFIGs are important for voltage stability studies of the wind power system. Currently, there is no standard model for the DFIG that can represent

a large wind-dominated power system. However, the models used for stability studies should encompass all major components of the wind turbine generator. Also, it should include the control circuit with the aerodynamics of the WTG. The schematic of the DFIG has been presented in Fig 3.8 with Z_{eq}/s is the equivalent impedance. The power transferred by the air gap to the stator at unity power factor is :

$$P_{ag} = \frac{\omega_s T_m}{p} = 3(V_s - I_s R_s) I_s \tag{3.32}$$

In this equation, ω_s represents the stator synchronous speed, V_s denotes the stator voltage, the stator winding resistance is R_s, the number of pole pairs is p while the mechanical torque T_m being computed as follow:

$$T_m = \frac{P_t}{\omega_r} \tag{3.33}$$

ω_r denotes the rotor speed. by replacing this value of T_m in the Eq 3.26, we have :

$$I_s = \frac{V_s \pm \sqrt{V_s^2 - \frac{4 R_s \omega_s P_t}{3 P \omega_r}}}{2 R_s} \tag{3.34}$$

The stator current I_s and the rotor voltageV_s can be computed by using the Fig 3.5. The voltage across the magnetizing branch of the steady-state model is :

$$\overline{V_m} = \overline{V_s} - \overline{I_s}(R_s + j\omega_s L_{ls}) \tag{3.35}$$

L_{ls} is the stator leakage of the DFIG. The magnetizing current can be computed by using the equation.

$$\overline{I_m} = \frac{\overline{V_m}}{j\omega_s L_m} \tag{3.36}$$

The magnetizing inductance is L_m and the rotor voltage and current can be computed by :

$$\begin{cases} \overline{I_r} = \overline{I_s} - \overline{I_m} \\ \overline{V_r} = s\overline{V_m} - \overline{I_r}(R_r + js\omega_s L_{lr}) \end{cases} \tag{3.37}$$

R_r is the resistance of the winding,L_{lr} is the rotor leakage inductance and s is the slip that can be computed as follow.

$$s = \frac{\omega_s - \omega_r}{\omega_s} \tag{3.38}$$

3.6.2 Wind Farms Model for the Power Flow Analysis

During the planning and design stage of a wind-dominated power system, for security and reliability purposes, it is vital to include the wind farm in the load flow studies. Transmission planners and designers use the two well-known methods PQ and RX bus [30],[40]. The PQ bus model assumes that real power and its power factor are known and the reactive power associated is computed. The reactive power consumed

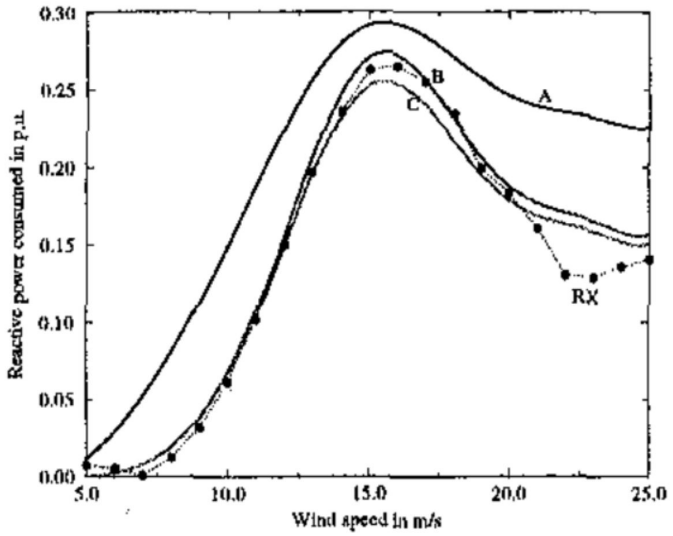

Figure 3.11: Reactive power of WT Vs wind speed [17]

the wind turbine generator is a function of its real power consumed and can evaluated

by [8]:

$$Q = -Q_0 - Q_1 P - Q_2 P^2 \tag{3.39}$$

Q_0,Q_1,Q_2 are experimentally computed. The reactive power of the wind farm is approximated as :

$$Q \approx V^2 \frac{X_c - X_m}{X_c X_m} + \frac{X}{V^2} P^2 \tag{3.40}$$

3.7 Traditional Power Systems and their Voltage Stability

Voltage stability is not a new phenomenon in the electric utility industry worldwide. Researchers and scholars around the world are now devoting a lot of attention to this problem to come up with novel solutions. Primarily, voltage stability problems were related to weak transmission grids and long transmission lines. Now, in today's competitive world, power is being operated close to its limits. Several recent major blackouts in the world have been initiated by voltage instability which stressed the importance of operating the power system in a stable mode [18]. The power system is the most complicated man-made system. Operating a complex system of this type in a stable manner is not facile. Its stability depends mainly on the topology of the grid, operating conditions, and disturbance.

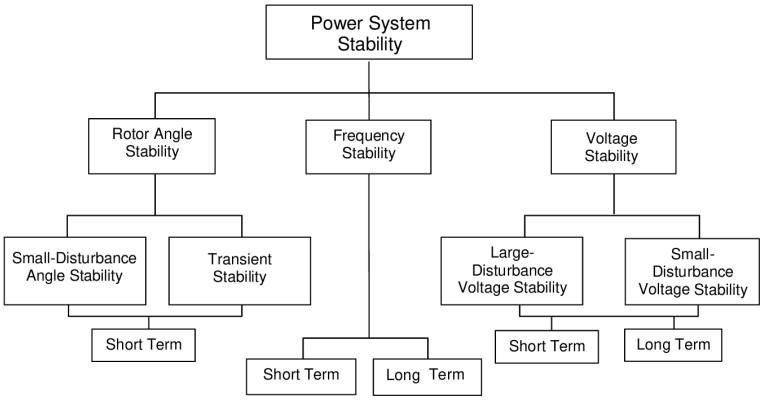

Figure 3.12: Categorization of power system stability

3.8 Effects of Wind Farms on Voltage Stability of Traditional Power System

Due to climate change, the power system industry is under tremendous changes from a political and technical standpoint [2]. The traditional power system is subjected to enormous integration of wind energy year by year. A lot of works has been done on how wind farms can negatively impact grid voltage stability. Prior works done pointed out that power systems with wind levels penetration higher than 30% can negatively affect the voltage stability. Because of their inherent nature, large wind can be the source of some major challenges to the transmission system operators [32].

1. Fluctuation of the power generated: The wind velocity is constantly changing so does the output power of the wind farm. As a result, satisfy the load balance equation is a complex task.
2. Intermittency and load mismatch: The wind turbine power output is imposed by the velocity of the wind that leads to mismatch power in the power system.
3. High demand for reactive power: Wind turbines use induction generators to produce electrical energy; reactive power is needed for excitation. According to wind farm operators, wind farms could cause the following voltage issues [12],[14].

   – Voltage fluctuation at the PCC – Voltage sag or rise.

   – Voltage asymmetry and flicker – Voltage collapse

In Denmark, a world leader in wind energy, a study has been done to integrate three 150 MW offshore wind farms during 2002-2008. The results of the study showed

that wind farms could harm the voltage stability and power of the Danish grid. Additionally, it has been found that an eventual three-phase fault at any bus of the grid can trigger its voltage collapse without any Remedial Actions Schemes. Also, the total power loss of the grid has been increased by 32 %.

Germany, another world leader in wind energy, stability, and transmission congestion were a major concern for transmission system operators. Some transmission lines of the German grid have been already overloaded especially in the North where Germany shares the border with Denmark. I n that case, to prevent the voltage collapse, the power grid operator was obligated to curtail the wind power flow into the German grid. To manage the matters related to the dynamics characteristics of wind turbines and voltage stability, Germany has implemented strict codes. The impossibility to satisfy the equation supply-demand and intermittency of wind energy are urgent challenges for transmission systems operators. The worst-case scenario is when a massive wind capacity is disconnected from the transmission by the protection and control system amid a three-phase short circuit. This situation can create a lot of problems related to voltage instability and frequency or eventually drive the system into voltage collapse. Having said this, keeping voltage stability and frequency stability in wind-dominated power systems is burdensome. Beyond any doubt, research related to the impacts of wind farms on voltage stability will be an active area of research in power system engineering. Because of competition in today's deregulated electricity market, transmission grid operators are operating their grid to maximize their profits and hence create transmission congestion problems. Novel Market design to accommodate high wind penetration levels into the transmission will need also to be researched.

3.9 Traditional and Modern Solutions to Improve Voltage Stability

Several symptoms can provide a good intuition to the power grid operator about voltage instability issues. Among them are low voltage profile, high active power loading of the power system, insufficient reactive power resources. When happened, voltage instability has several detrimental consequences like long system restoration and privation of a large group of customers from electrical energy. Actions schemes to mitigate voltage need to consider the symptoms to design the best approach to take corrective actions. Some of the corrective actions will be described in this section.

1. Load Tap Changer control modification: The LTC of the power transformer can be detrimental to the voltage stability of the power grid. To counter these issues, several modifications can be done in the LTC. The tap changer might be locked on the actual tap to prevent voltage magnitude decline. One can also reduce the set of the LTC controller. The restoration of the voltage on the HV side might be reversed by the logic controller in place of the LV side. The load side voltage can be reduced which will decrease the load on the transformer [21].
2. Load shedding Technique : Load shedding is a technique used by transmission grid operators to keep the power system stability by disconnecting the overloads in some regions of the power system. Although this practice creates discomfort for customers, it is very efficient to prevent voltage instability or even voltage collapse. Successive load shedding is performed by the grid operators to bring back the voltages profiles of the power system to acceptable limits. This technique is a cost-effective solution and is easy to implement. However, since electricity is a commodity like air and water for modern society, customers will be penalized due to load shedding. Thus, this measure should the last measure to be taken by the grid operator to save the power system from voltage instability [21].

3. Action on Generators : Reactive power compensation devices and generators are important in controlling the voltage of the power system. During peak load conditions, capacitive compensation devices are switched ON whereas induction compensation devices are switched OFF. The voltage set point of the generators might be augmented to decrease the current of the transmission system. This technique works if and only if the load can be more or less modeled as a constant power load. Consequently, the LTC of the power transformer should be in operation. Some conventional power could be commissioned to help to balance the load of the system. Quick starting units are used to meet the peak demand of the power system. However, generation rescheduling is complex and requires thorough approaches, and need time to be implemented.

Some contemporary trends in the power industry to counter the voltage collapse is stressed in the followings lines.

1. Reactive power compensation with the proper selection of compensation schemes with the right size, rating, and placement, the voltage stability margin can be augmented [37].
2. Coordination of protections and controls: Proper coordination should be used among protections and controls according to simulation studies. Tripping of the elements of the power system should be the least measure to save the power system from instability
3. Operator's roles: Possible symptoms related to voltage instability should be identified by the control room operator to take action accordingly. In that sense, real-time monitoring and analysis are crucial.

The control room operators should be able to identify voltage-related symptoms and act accordingly to prevent voltage collapse. Potential

stability problems could be detected by using Online monitoring tools so that the Remedial Actions Schemes (RAS) can be taken.

Chapter 4

Voltage Stability of Grid-connected Wind Power Plants

The focus of this section is to present the use of some popular FACTS devices such as STATCOM and the SSSC to ameliorate the stability of power grid.

4.1 Introduction

With the menace of climate change, policymakers worldwide are investing in renewable energy resources. These two energy sources are free and almost without pollution. In the last decades, an enormous amount of wind energy has been integrated into the transmission grid. However, renewable energy is not a cure-all remedy since they pose several challenges to transmission systems operators. The grid operators are facing several majors challenges to meet reliably their load demand. Keeping the system security intact, power quality issues combined with stability issues are among the major challenges of today's Transmission System Operator [3]. As voltage stability is a static phenomenon, steady-state voltage stability has been proposed to evaluate the security margins of the power systems. The concept of QV instability will be detailed accompanied by the impacts of different parameters on the QV instability. A method to interconnect the new wind farm with the transmission grid to ameliorate steady voltage stability will be presented. Lastly, FACTS devices such as STATCOM, SVC devices can be integrated into the power system to augment the transfer margin of the transmission grid.

4.1.1 Wind Generator Voltage Control Strategy and Voltage Stability

Conventional synchronous generators, traditionally, can be operated at voltage constant mode or power factor control mode. Each mode of operation has its merits and

depends upon the needs of the system. similarly, modern wind turbines can be operated in different modes to regulate the voltage of the grid. For instance, the operation of the DFIG at a low power factor has more benefits for the reactive support of the transmission grid [4]. In so doing, the closest area of the power system to the wind farm will witness an increase in the QV-stability margin. Nevertheless, a generator can provide constant active power output in power factor control mode independently of the transmission grid conditions. As a result, the DFIG will not be able to assist the grid in reactive power injection. Voltage control mode can be implemented in the DFIG to alleviate this issue. In that mode of operation, the double-fed induction generator maintains the terminal voltage constant by adjusting its reactive power output according to its capability chart [10]. However, to be pragmatic, this strategy might be suitable while considering the grid code requirements. Other control strategies exist to assist the power grid in terms of reactive power support. However, the best control strategy should include cost optimization and feasibility while considering the grid codes requirements [16],[17].

4.1.2 Reactive Power Capability of DFIG amid Fault Conditions

During a short circuit from the external grid, modern wind turbines can assist the grid in reactive power support to meet the grid codes requirements imposed by the power grid operators. In that sense, the wind turbine can ride through the fault to meet the requirements imposed by the transmission system operator. Using mechanical switched capacitors banks to inject reactive power into the grid for voltage reactive power support is not a practical solution since the banks would switch too many times. Other approaches by using more sophisticated compensation devices are used by the power grid operators. After clearing the fault, these compensating devices help to maintain the power system voltage stable. Transmissions System Operators have come up with mandatory requirements to keep the wind farm online during faults. Grid codes are mandatorily imposed by the transmission system operators so

that the power system can stay voltage stable during a fault. The most important requirements of these grid codes are [33],[38],[43]:

- The capability to ride through faults from the external grids
- The capability to regulate the frequency and the active power fed to the grid
- The capability to regulate the reactive and the voltage at the point of interconnection
- Frequency and voltage operation range

During steady-state operation conditions, the wind farm draws power from five regions which will be described later in this work. Furthermore, during a fault from the external grid, several controls strategies are deployed to keep the wind turbine Online. One of these is short-circuiting the rotor circuit. In turn, we limit high values of current flowing through the stator. As a result, we protect the side containing the generator and converter. In addition, we bypassed current flowing into the rotor by connected the winding of the rotor with a set of resistors. This is referred to as the crowbar system [43],[26]. The active and the reactive power can be regulated by adjusting the stator and the rotor current.

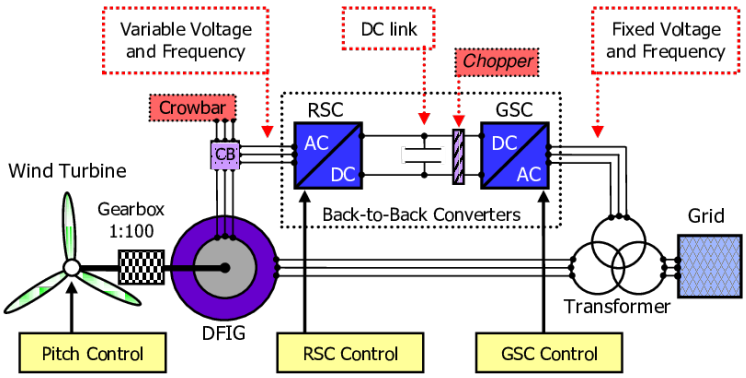

Figure 4.1: DFIG wind turbine power grid connection [43]

For a DIFG, based on aerodynamic data on wind velocity, there is wide range of variation of active power.

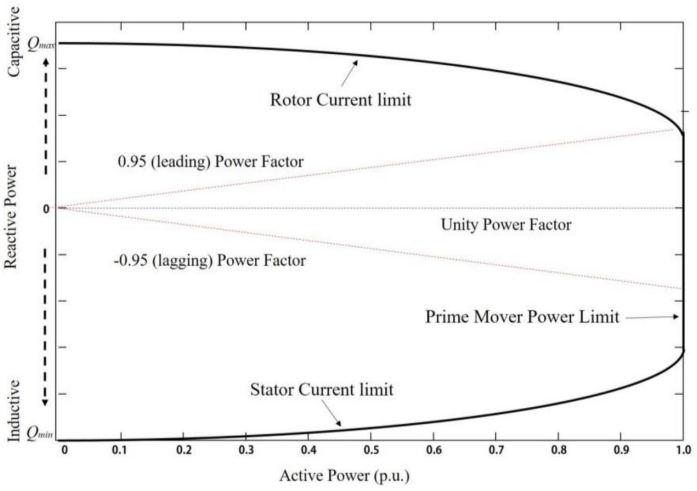

Figure 4.2: Curve of the reactive power capability a DFIG [43]

4.2 STATCOM Applications

The STATCOM is one of the sophisticated power electronics-based members of the family devices called FACTS. IGBT and GTO are utilized as forced commutated devices for power flow control in the STATCOM. They can consume or pump reactive power into the line [36], [37].

4.2.1 Working principles of STATCOM

The power transfer equation needs to be invoked to digest the working principle of the STATCOM. Let us suppose that we have two sources V_1 and V_2 connected via an impedance $Z = R + jX$.

For a transmission line, the resistance can be neglected in comparison to the reactance of the line and we have.

$$Q = \frac{V_2}{X}(V_1 \cos\delta - V_2) \tag{4.1}$$

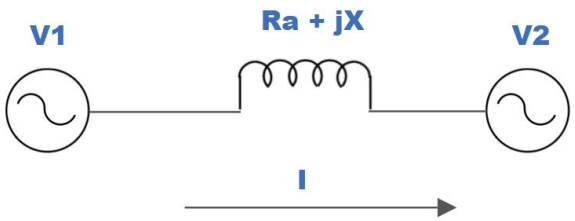

Figure 4.3: Two voltage sources connected via an impedance

δ is the difference angle of the voltages V_1 and V_2.

if $\delta = 0$ we have

$$\begin{cases} Q = \frac{V_2}{X}(V_1 - V_2) \\ P = \frac{V_1 V_2}{X} \sin \delta \end{cases} \tag{4.2}$$

It is blatant that if $\delta = 0$ the flow of active power is zero and the reactive power flow is a function of the difference $V_1 - V_2$.

The STATCOM is a fast-active device that injects or absorbs reactive current by controlling the voltage at the point to which it is connected to the power grid. Because of its fast response, this technology is very convenient to maintain voltage amid grid faults, ameliorating short-term voltage stability. The STATCOM has some other merits such as damping of low-frequency power oscillations, active harmonic filtering, and power quality improvements. The grid connection point voltage serves as a reference for the regulation of the voltage waveform of the STATCOM. The STATCOM supplies capacitive reactive power to the grid if the voltage amplitude of the STATCOM is larger than the voltage of the system. Otherwise, inductive power is supplied to the grid. How much reactive power can be supplied is a function of the short circuit reactance and the difference $V_1 - V_2$ and the thermal limits of the IGBTs. In steady-state operation, there is no reactive power exchange with the transmission grid.

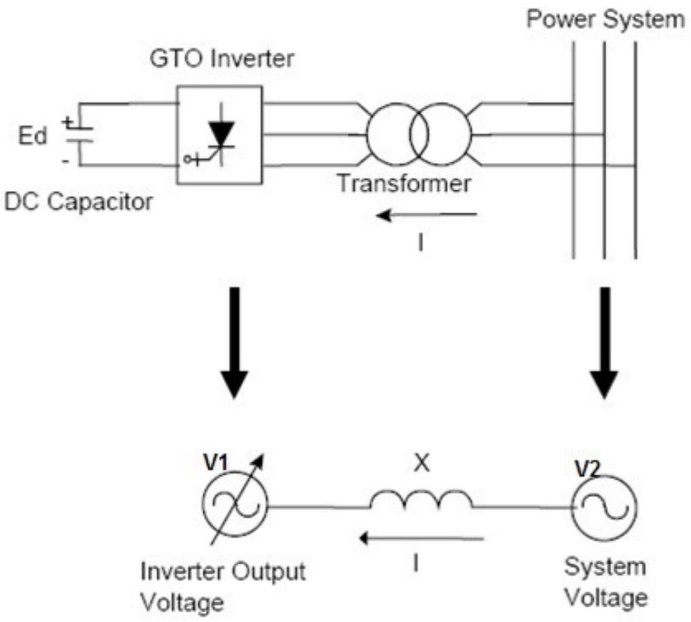

Figure 4.4: Electrical diagram of STATCOM

The following figure shows the two-mode of operations of the STATCOM

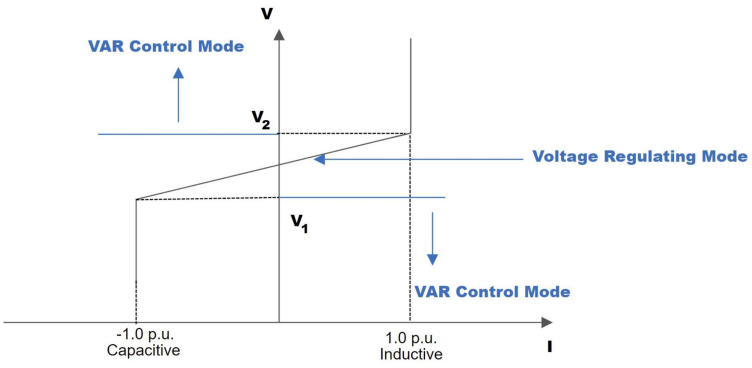

Figure 4.5: Operation modes of a STATCOM

It can be seen that the voltage regulation of the STATCOM is between $V_1$and V_2 if the transmission grid voltage is lower than V_1 or higher than V_2. In this case, the STATCOM operates in Var control mode.

4.2.2 Motivations for STATCOM

Voltage stability is an intense area of research in power systems. Research engineers are busy developing the best techniques to mitigate this phenomenon. Today, the

power system is being increasingly stressed due to the greater demand for electrical energy. It is burdensome to acquire new Right Of Way of new transmission lines. Because of the competition initiated by the deregulation of the electricity market, transmission lines worldwide are heavily stressed. To augment the transfer capability of the transmission grid, sometimes, series and shunt reactive power compensation are used. The output power of the wind farm and the total demand load demand fluctuates constantly. STATCOM is installed to keep the voltage magnitudes in the permissible ranges. The STATCOM can participate in the Low Voltage Ride Trough requirements since it can operate at full capacity and extremely low voltage.

4.2.3 STATCOM Modeling

A STATCOM comprises a coupling transformer, a VSC, and a DC energy storage device. It is a very sophisticated FACTS device that can provide ease of voltage control, quick dynamic response, voltage support for changing loads conditions in a grid. A functional model of a STACOM is shown in Fig 4.6.

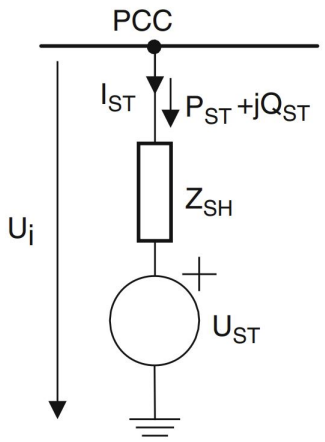

Figure 4.6: Equivalent circuit diagram of the STATCOM

The voltage of the VSC has the same frequency as the grid voltage and has a controllable amplitude and phase. Moreover, a filter and a transformer are sued to

connect the VSC to the grid. The STATCOM regulates the voltage of the bus with respect to the magnitude voltage of the VSC. The terminal bus voltage is obtained by the addition of the voltage of the output voltage of the converter and the leakage voltage of the inductance $V_{STATCOM}$. The current fed into the grid by the STATCOM ensures the reactive power exchange with the grid. The block diagram control of the STATCOM in DigSILENT Power Factor is presented in Fig 4.7. The STATCOM

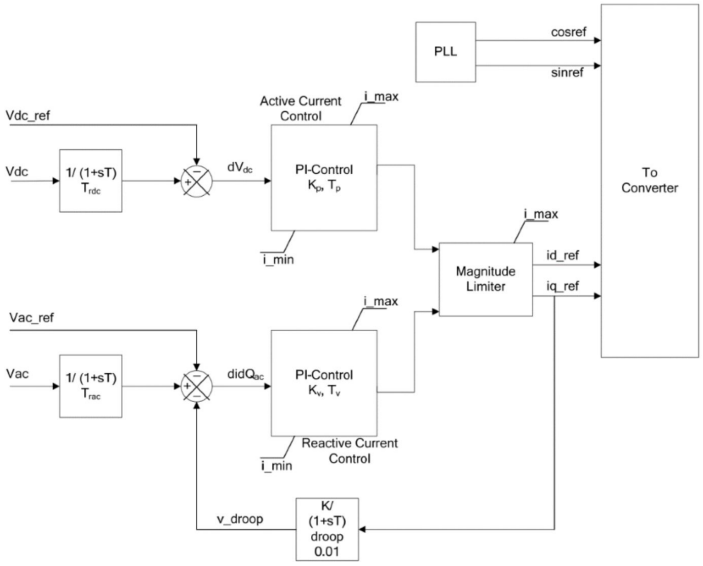

Figure 4.7: Operation modes of a STATCOM

can provide reactive power support by continuously changing its susceptance whilst providing a fast voltage support response at a local node. In the d_q frame, the outputs of the controller are i_{dref} i_{qref} which are required to calculate the power transferred by the STATCOM to the grid .

$$\begin{cases} P_{inj} = V_i(i_d \cos\theta_i + i_q \sin\theta_i) = v_d i_d + v_q i_q \\ Q_{inj} = V_i(i_d \sin\theta_i - i_q \cos\theta_i) = v_q i_q + v_q i \end{cases} \tag{4.3}$$

The power and the current injected by the STATCOM are the controlled variables. The rating of the STATCOM is done by considering several parameters such as the amount of reactive power needed to recover and survive during major disturbances.

4.2.4 Location of the STATCOM

To better support the transmission grid in reactive power supply, grid operators place the STATCOM by considering its effects on the stability during heavy load conditions. The SATCOM can effectively support the voltage of the system when placed as close as possible to the load bus. Also, it improves the transfer capability of the system. During a fault from the external grid, STATCOM, if placed at a suitable location can help in keeping the wind farm online.

4.2.5 Static Synchronous Series Compensator (SSSC)

The SSSC is extensively used to regulate the power flow through the transmission line and also to damp the oscillations of the power system after a fault. The SSSC can behave as reactive or inductive inductance to control the power flow through the line.

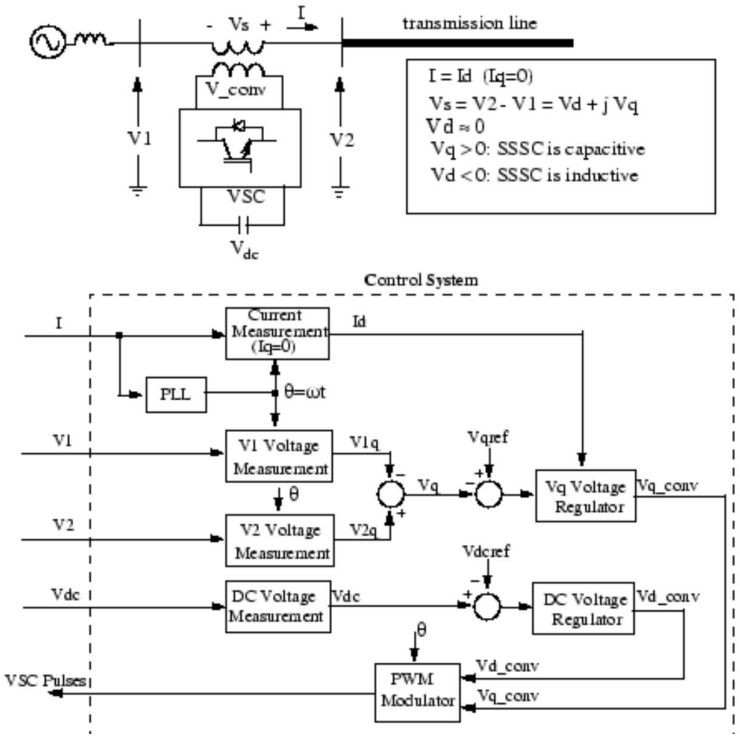

Figure 4.8: Block diagram of a SSS [48]

4.2.6 Sizing of the SSSC

New Right Of Ways (ROW) for transmission lines are complicated to acquire. Electric utilities worldwide are busy trying to find how to optimally exploit their existing lines. To do so, they use the FACTS devices to control the power flow through the lines. One of the most used FACTS devices is the SSSC. This fact device can control the power flow through the line and can damp the oscillations of power in the system after a fault. To size, the SSSC, the maximum line current combined with the desired voltage is used. The proper rating of the SSSC is computed as follow :

$$SSSC_{Rating} = \sqrt{3} I_{Max} V_{SSSCMax} \tag{4.4}$$

In this work, the optimal rating capacity of the SSSC is not computed. As a result, the SSSC might be oversized, in simulation, to keep the injected voltage 10 percent of the voltage nominal. In this work, the SSSC is connected in the middle of lines 1 to 2 to appreciate its effects on the critical clearing time.

4.2.7 Cascading

NERC, the North American Electric Reliability Corporation, defines cascading as successive loss of major elements of the power system in an uncontrollable manner after a disturbance. From the Reliability Guideline of NERC, there are two types of cascading.

1. **Bounded Cascading**

   This type of cascading stops immediately on the removal of some component of the system to save the power system from a major blackout.

2. **Unbounded Cascading**

   This type of cascading is the most harmful to the power system. During an unbounded cascading, elements of the power system are removed after

driving the system into an unstable condition. The cascading events might lead to a blackout.

4.3 Critical Fault Clearing Time

CCT is vital in maintaining the system transient stable. In simpler words, critical clearing time is the time that is required by the protection control system to clear the fault before losing synchronism in the system [35]. The removal of the fault beyond the CCT might drive the system into instability. As a function complex function, the CCT depends on several parameters such as the pre-fault system conditions and post-fault conditions. The post-fault conditions are more or less a function of the protective relaying schemes of the power system. Trial error and error analysis of the post-disturbance equation of the system can be used to evaluate the CCT. The other approach is to integrate fault-on equation while checking if the Lyapunov energy function reaches its predetermined critical level [44].

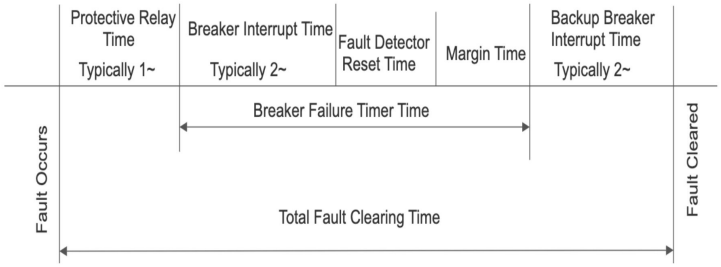

Figure 4.9: Total clearing time diagram [44]

An approximated value of the CCT can be calculated by.

$$\dot{s} = \frac{1}{2H}\left[T_m - T_e\right] \tag{4.5}$$

If the terminal of the generator is short-circuited we can write: $T_e = 0$ and then

$$\dot{s} = \frac{1}{2H}T_m \tag{4.6}$$

and by integrating both side eq 4.6 we can write.

$$\int_0^t \frac{1}{2H} T_m + s_0 \tag{4.7}$$

If the critical speed of the machine is s_c, we have :

$$t_c = \frac{1}{T_m} 2H(s_c - s_0) \tag{4.8}$$

The critical voltage is derived from the PV curves considering the maximum laodability of two areas of the power system. This can serve as an indicator to the power system planner for the protection against voltage collapse.

Chapter 5

Results and Discussions

5.1 Introduction

This section deals with analysis and discussions related to the simulations performed on the test system. The test system is modeled in DigSilent Power Factory and PSAT for analysis. The voltage security assessment of the test system is done at different wind penetration levels. An iterative approach is used to evaluate the safe P-Q regions of the test system as the wind penetration power penetration levels vary. Furthermore, the effects of the STATCOM on the amelioration of the transient stability under the assumption of a three-phase fault at the PCC are investigated. Furthermore, the role of the SSSC in damping the oscillations of the power system during post fault conditions is demonstrated. In addition, several contingencies are examined and the voltage security of the power system is assessed to determine the power curtailment from the wind park to the system voltage stable. The IEEE-14 bus was selected to perform the simulations and it comprises five generators with type-1 exciters, 11 loads. Among the generators, three of them are synchronous compensator that are used for compensation.

5.1.1 IEEE 14 Bus System

For simulations and analysis, the IEEE 14 bus system is selected. As a fraction of the United States of America power grid, the IEEE-14 bus system comprises fourteen buses or nodes, five generators, sixteen lines, eleven loads, five transformers, and a shunt. This system has no line limits and the slack bus is bus 1.

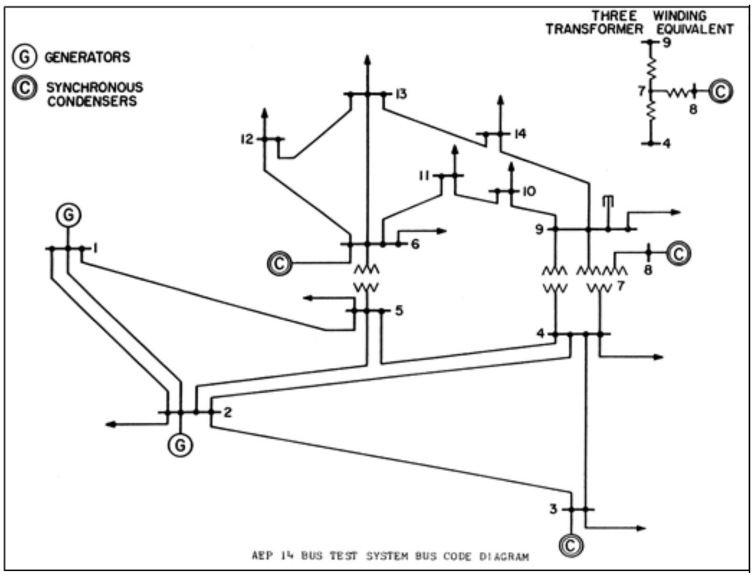

Figure 5.1: one line diagram of the test system

Before the modification of the test system, the power flow has been carried out in DigiSilent to have the pulse of the system. The test has all its buses voltage within the design limits. As can be noticed, Bus 3 shows the lowest voltage magnitude level and bus 8 the highest. Despite that bus 3 shows the lowest voltage level, it is erroneous to conclude it might be the strongest bus. Similarly, despite showing the highest voltage magnitude, bus 8 is not the strongest bus of the system.

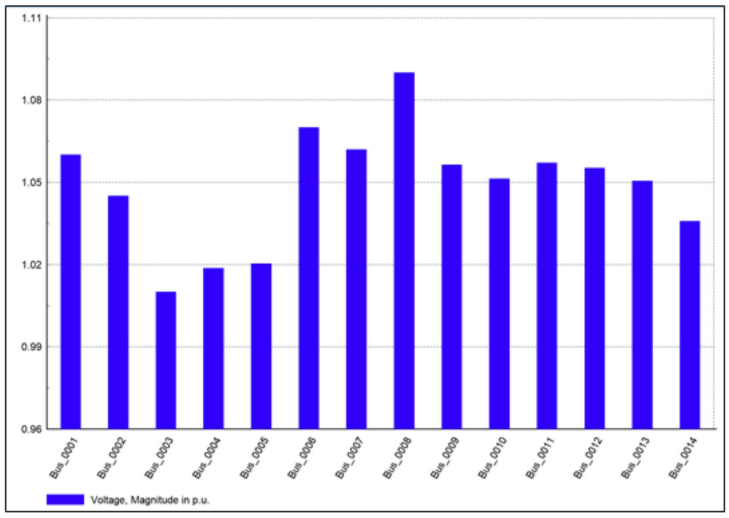

Figure 5.2: Voltage profile of the test system

5.1.2 Strength Assessment of the test system

For the operation and the planning of the power system, the assessment of its strength is of the utmost importance. One of the classic ways to evaluate the strength of the power is to use the PV curves. Indeed, this curve shows the variation of the voltage of the power system for different loading conditions [18]. Also, under various loading conditions and wind penetration levels, the QV curve is invoked to portray the stability levels of the system. To do so, the Reduced Jacobian matrix can be used, with greater precision, to detect the weakest or the strongest area of the power system. By invoking the QV modal analysis, the strength of the system is assessed and the results are presented in Table 5.1

Table 5.1: Eigenvalues of the reduced Jacobian Matrix of the system

Bus	1	2	3	4	5	6	7	8	9
Eigenvalue	65.09	39.02	21.69	18.85	16.30	11.21	2.69	5.52	7.60

The lowest eigenvalue is used for the participation factors computation. For this purpose, the PSAT toolbox is used and the participation factors are presented in the figure below.

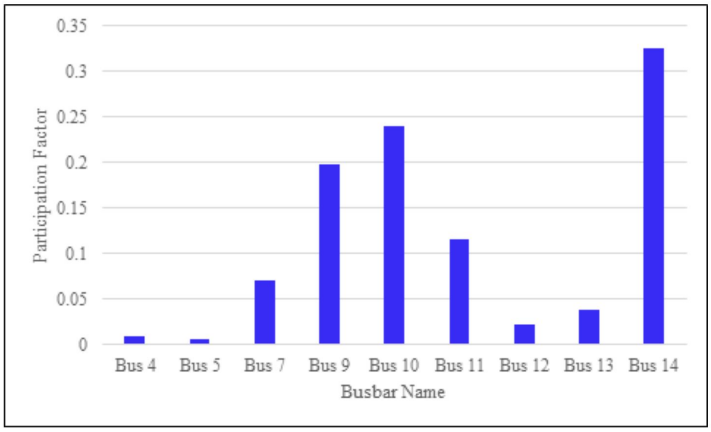

Figure 5.3: Bus participation factors of the test system

It can be noticed that buses 9 and 14 have the highest participation factors. Hence,

bus 14 is more vulnerable to voltage instability while bus being the most voltage stable bus.

5.1.3 Voltage Stability Margin(VSM)of the test system

Normally, the buses of the power system are restricted to stay inside a defined interval during its operation. The Voltage Stability Margin, which is a metric to assess the distance between the operating point of the power system and the maximum loading condition, is widely used for the voltage stability assessment [18]. Power systems with low voltage stability margins are more vulnerable to voltage instability [20]. In this work, the VSM is computed using the PSAT toolbox and we have:

Table 5.2: Voltage Stability Margin Busbars IEEE 14 bus

Bus	4	5	7	9	10	11	12	13	14
VSM	0.993	1.031	0.975	0.908	0.884	0.804	0.940	0.801	0.795

5.1.4 Proposed Analysis Method

An overview of the procedure invoked to detect the weakest and the strongest area of the system is presented. The IEEE14 bus system is used for simulation and it has been subjected to some modifications for the needs of the thesis. The test system is going to be simulated for PV curves analysis and QV curves analysis. Based on these results, the weakest of the system is depicted and is selected for reactive power compensation.

In this work, a weak area of power is the one that is incapable to meet its reactive power demand [18]. Reactive power compensation is generally, used to improve the loading of a weak bus. The element in the Jacobian matrix that shows the highest value for the reactive power sensitivity with resepct to the voltageis the most vulnerable to voltage collapse. The results above can be

served for the siting of a new wind farm under the constraint of not deteriorating the

voltage stability. The iterative approach called the brute-force method is invoked to find the appropriate location of the wind farm.

5.1.5 Scenario 1

In this scenario, a SSSC is included between line 1 and 2 the magnitude of its voltage is variable. The SSSC , as outlined, can imitate a capacitive and inductive reactance. The voltage is varied from $-0.20p.$ to $0.042p.u$ by an imitation of a capacitive and reactive reactance respectively as follows. First, the voltage $V_{ref} = 0p.u$ at $t = 2s$. Then after, $V_{ref} = -0.2p.u$ and at $t = 6s$ $V_{ref} = 0.042p.u$. Secondly, a 150 MVAR STATCOM is included at bus 2 in Var control mode. $I_ref = 0$ at $t = 2s$ and STATCOM set $I_{ref} = -1p.u$ in capacitive mode.After $t = 6s$, $I_{ref} = -1p.u$ has been set to inductive to regulate the reactive power injection to the power grid

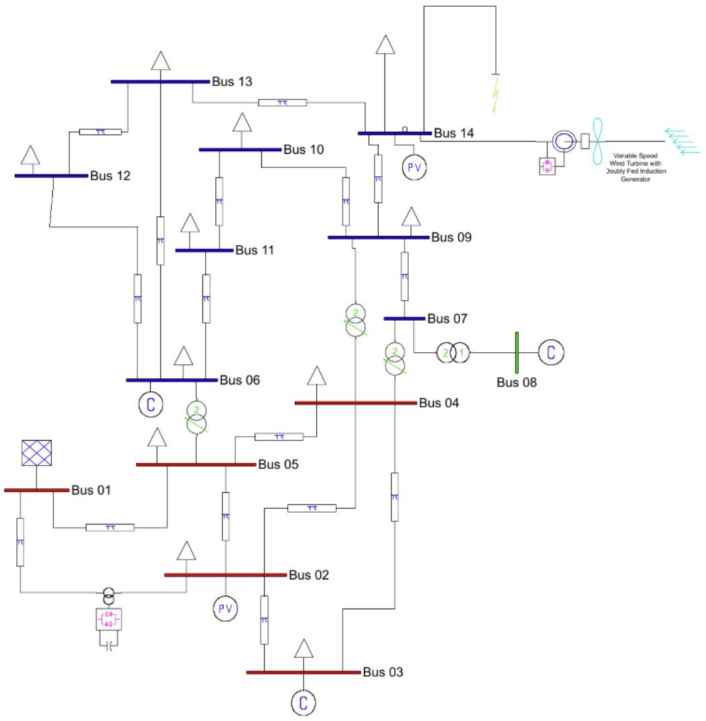

Figure 5.4: One line diagram of the test system with the SSSC

To illustrate the effects of the addition of the SSSC and the STATCOM, the voltage magnitudes and the power flow at buses 2, 4, 13 are shown in the table below.

Table 5.3: Power flow with and without FACTS

	No FACTS		**With SSSC**		**With STATCOM**	
	Total Generation	Total Loss	Total Generation	Total Loss	Total Generation	Total Loss
Active Power	3.82	1.24	3.80	1.11	3.82	1.13
Reactive Power	2.18	1.37	2.11	1.39	2.07	1.41

The following table presents the voltage magnitude at bus 2,4,13 with and without FACTS devices.

Table 5.4: Voltage magnitudes with and without FACTS

Bus Name	**No FACTS**	**With SSSC**		**With STATCOM**	
		Capacitive	Inductive	Capacitive	Capacitive
Bus 2	1.055	1.085	0.987	1.045	1.013
Bus 4	1.022	1.042	0.975	1.050	0.988
Bus 13	1.067	1.075	1.037	1.051	1.049

The results above have demonstrated that the SSSC included between lines 1 2 can regulate the buses voltage of the test system and the total loss has been considerably reduced. However, the STATCOM has no significant effect on the total power losses. During the $N-1$ condition, the line between busbar 2 and 4 is removed and the power flow is done. The reason behind this action is to check for congestion which is the situation where the transmission lines are incapable to accommodate all loads during peak demand or emergency demand like $N-1$ or $N-2$ or worse. I t is worth reminding that grid congestion affects the reliability and efficiency of the transmission lines. Furthermore, it impacts the electricity market operations since retailers may not access the cheapest energy source. Following the Blackout 2003, the energy policy act 2005 established a mechanism to help ameliorate the efficiency, reliability, and capability of the grid. The Contingency Analysis has been done and all lines and the voltage at each bus are checked and the results show that the test system is $N-1$ secure. To demonstrate the impact of the SSSC on the critical clearing time improvement, some buses of the power system is faulted.

Table 5.5: Critical Clearing Time (CCT)

Faulted Bus	No FACTS	With STATCOM	With SSSC
Bus 2	0.378 s	0.427 s	0.456 s
Bus 4	0.425 s	0.489 s	0.539 s
Bus 6	0.695 s	0.749 s	0.778 s
Bus 8	0.787 s	0.845 s	0.788 s

The SSSC has more efficiently impacted the CCT of the system in a sense that the CCT with SSC is better than the one with the STATCOM. Despite the fact that the STATCOM can be used for CCT improvement and for voltage regulation, the SSSC is more effective in improving the the critical clearing time of the system.

5.1.6 Scenario 2

The effects of the STATCOM in supporting the grid in reactive during a fault at the PCC are demonstrated. Most grid code worldwide considers the aforementioned fault as part of their FRT. The fault applied at the buses is cleared after 5 cycles. Furthermore, the voltage at bus 14 during the fault, the voltage recovery time, and the settling time are analyzed and compared.

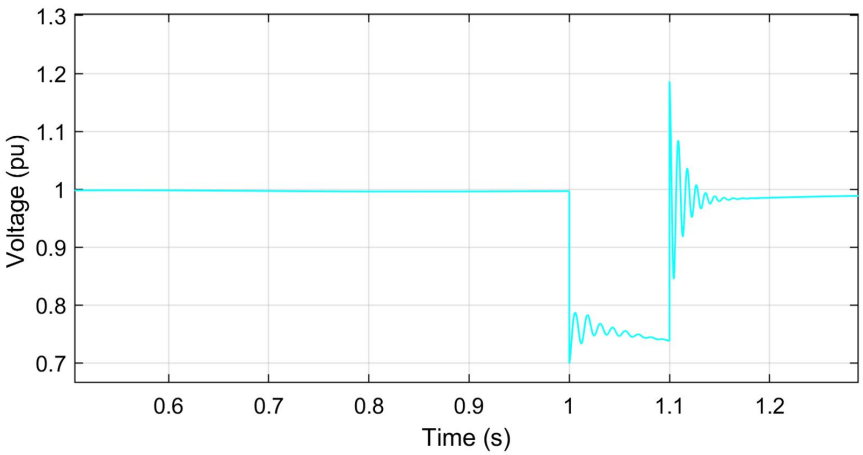

Figure 5.5: Voltage at the POI without STATCOM

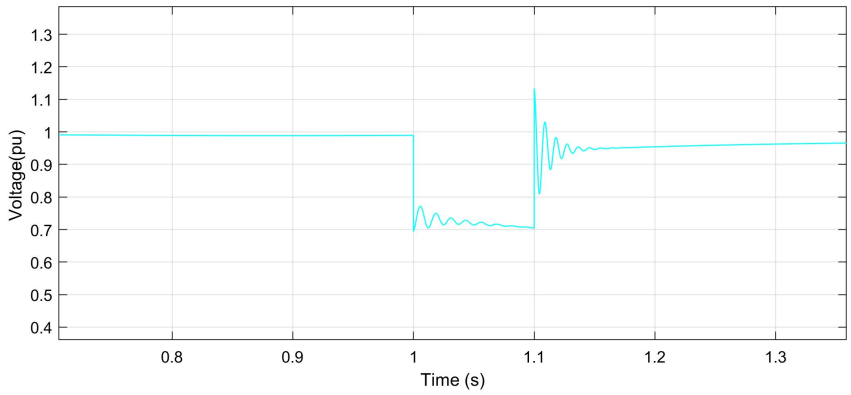

Figure 5.6: Voltage at the POI with STATCOM

When the fault has initiated the voltage at the PCC drop to almost zero since the electromagnetic torque of the wind turbine generator has been considerably reduced. Once the fault is cleared, the rotor speed increases, and the wind turbine generator consumes a large amount of reactive power. This leads to voltage stability problems. Without any proper control actions, it might be burdensome to bring back voltage to the acceptable interval. It is blatant the wind farm does not meet the FRT requirements that stipulate the wind farm should be kept **Online** for voltage lows as 5% of the nominal value for up to 250 ms. This type of behavior of the wind farm amid a short circuit is undesirable from a transmission system operator's point of view since it drives the entire grid into instability. To overcome this drawback and keep the wind farm **Online**, a STATCOM is connected at bus 14. Fig 5.2 shows the LVRT of the WT in the presence of a Three-phase fault at the PCC.

After the removal of the fault,the active power oscillates for a long period before reaching its steady-state **value. The** same scenario is also valid for the reactive as one can depict in the following picture.

From Fig 5.4, with the STATCOM the wind farm exhibits a better performance in the presence of a three-phase fault at the PCC.

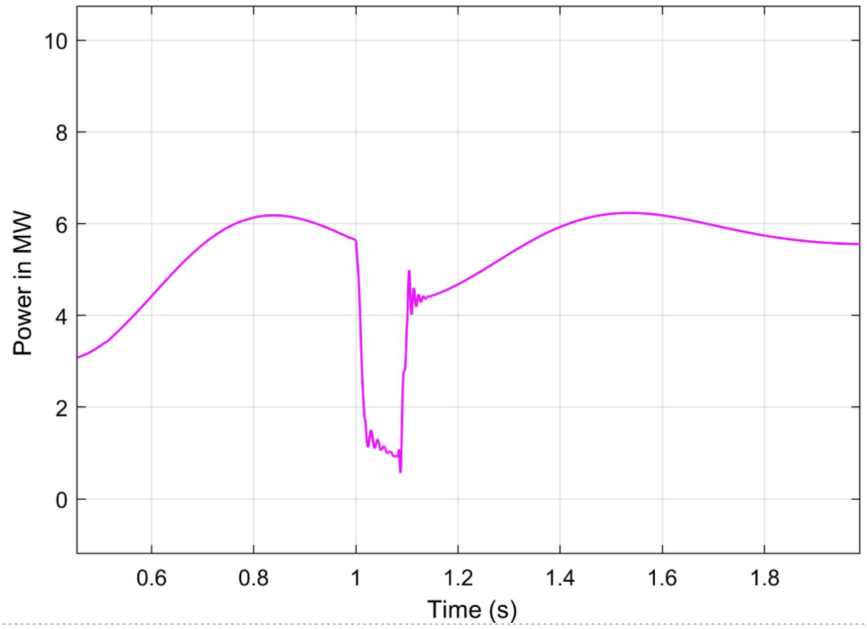

Figure 5.7: Wind Farm active power output at PCC without STATCOM

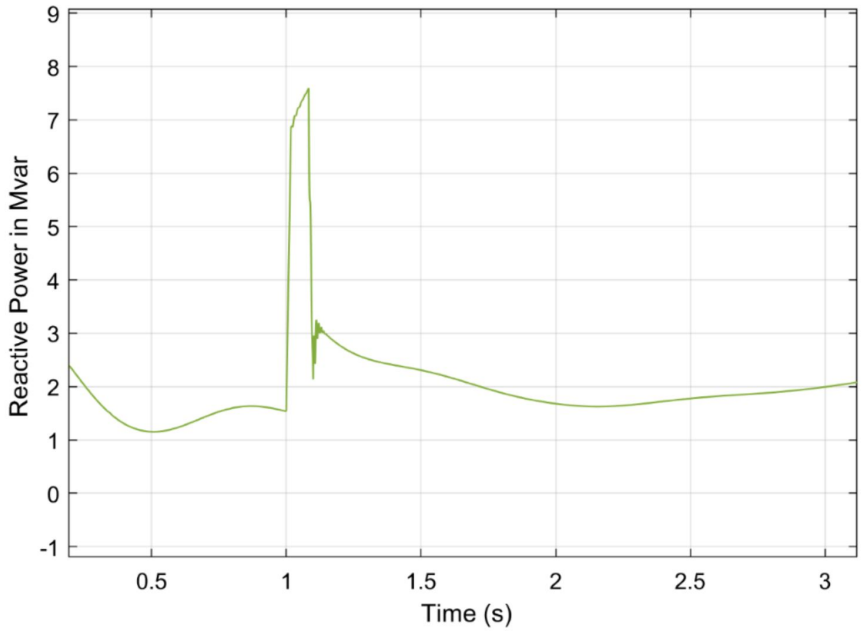

Figure 5.8: Wind Farm reactive power output at PCC without STATCOM

5.1.7 Economic Feasibility of LVRT Solutions

Installation cost and operations cost are the main components of the cost function of FACTS devices. The initial cost encompasses the cost of the whole FACTS system

and delivery, installation cost, and taxes. The total installation cost of a FACTS device is a function of its rated power. The operations cost comprises maintenance cost and service, insurance, and taxes. It is estimated that the annual operations cost is approximately 5% to 10% of the initial cost. The figure below shows the typical cost structure for FACTS devices.

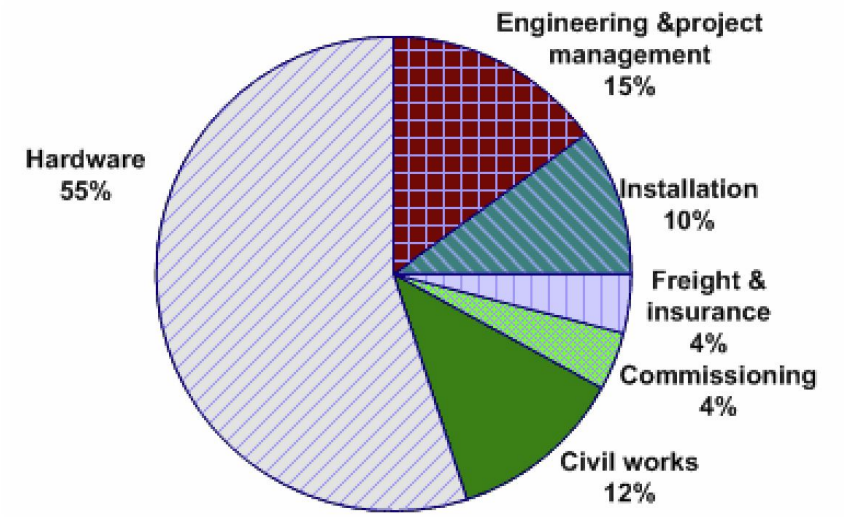

Figure 5.9: Cost structure of FACTS installation [49]

5.1.8 Price Guideline

FACTS devices use several expensive components for their manufacturing such as capacitor banks, reactors, thyristors, reactors, switchgear. Consequently, approximate the cost of a FACTS device is complex. For example, EPRI and Siemens use the following cost function to approximate the cost in US dollars of a STATCOM and SVC [49].

$$\begin{cases} COST_{STATCOM} = 0.003S^2 - 0.233S + 153.45 \\ COST_{SVC} = 0.003S^2 - 0.305S + 127.38 \end{cases} \tag{5.1}$$

In these cost functions S denotes the rated capacity of the STATCOM or SVC. Some reports use the table below to compute the basics prices of FACTS devices. For FACTS devices with rating comprised between 150kVAR and 500 kVAR, the prices can be approximated by using the Table below.

Table 5.6: Cost of FACTS [49]

STATCOM	$ 40 /kVAR
SVC	$ 35 /kVAR
UPFC	$ 40 /kVAR
TCSC	$ 50 /kVAR
PSS	$ 70 /kVAR

Table 5.7: Price of FACTS [49]

SIZE	**Cost in US/kVAR**
>500 kVAR	<179
100-500kVAR	179 - 299
<100kVA	>299

From table 5.7, the transmission planners can have an intuition about the possible cost of the LVRT solution envisaged. However, the final solution to the LVRT amelioration is not only guided by the cost of the FACTS devices. A thorough approach is needed for the final decision.

5.1.9 Scenario 3: Integration of the Wind farm at the Weakest Bus

This section deals with the identification of the maximum wind power that can be injected at the weakest bus of the power without the deterioration of the steady-state voltage stability. Several penetration levels have been used for the calculation of the QV stability margins associated. The nominal power of the wind farm is around 100 MW. Lastly, the QV curves are plotted for different wind penetration levels to portray the effects of the wind penetration level of transfer margins and steady-state voltage stability. This aspect is very important to assess whether or not the power system will remain voltage at the now wind penetration level.

The penetration levels that are used for the tests are : $60\%, 80\%, 100\%$. In the context of this work, wind penetration level is the ratio of the summation of the

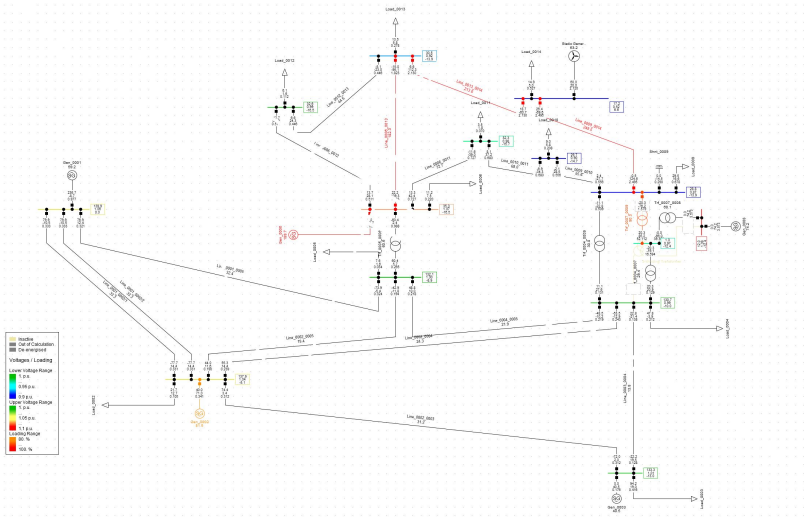

Figure 5.10: Single line diagram of the test system in DigSilent Power Factory

installed wind capacity and the total load.

$$Penetrationlevel = \frac{\Sigma InstalledWindCapacity}{\Sigma Load} \tag{5.2}$$

The transfer margin can be viewed as the ratio of the percentage increase in load (MW) and the base case power computed in the PV analysis.

$$TransferMargin(TM) = \frac{MW_{PV} - MW_{basecase}}{MW_{basecase}} \tag{5.3}$$

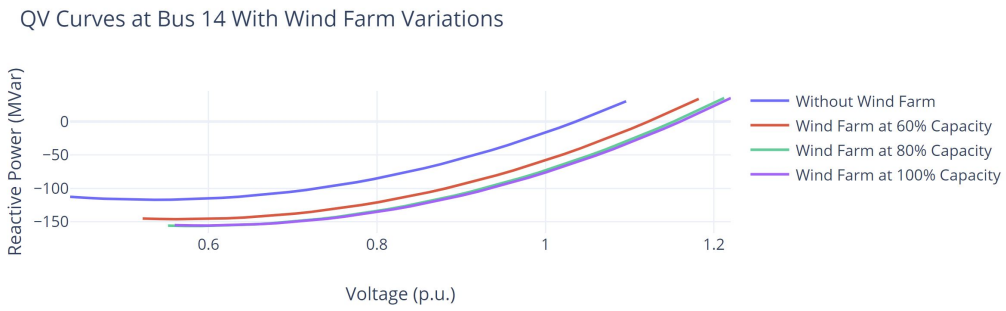

Figure 5.11: QV curves for Bus 14 with wind farm at Bus 14

The integration of the 100 MW wind farm at the weakest bus is more profitable for higher penetration wind power levels. While the power of the wind farm varies to 60%, 80%, 100% of its capacity, the QV stability margin is recorded each time.

Table 5.8: VQ stability margin bus 14 for wind farm power variations

Wind Penetration Level	QV Margins
0%	117.24 MVar
60 %	146.34 Mvar
80%	150.48 Mvar
100 %	155.35 Mvar

The importance of accurate model of the wind farm has been stressed for voltage stability studies.

5.1.10 Scenario 4: Integration of the wind farm at the Bus 5

For this study, a 100 MW DFIG wind farm is installed at bus 5 and QV margins of the other buses are computed.

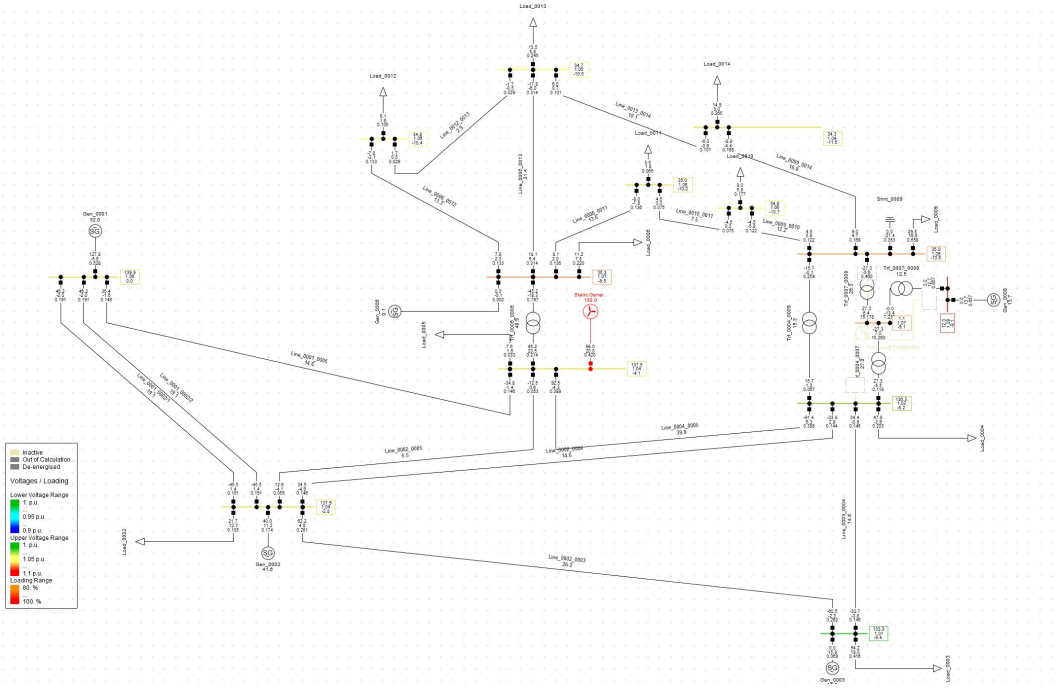

Figure 5.12: QV curves for Bus 14 with wind farm at Bus 14

The wind farm is integrated at the strongest bus of the system with the penetration level of the wind farm being varied. The tested penetration levels for the computation of the transfer margins are $60\%, 80\%, 100\%$. The QV curves are plotted for the wind corresponding wind penetration levels.

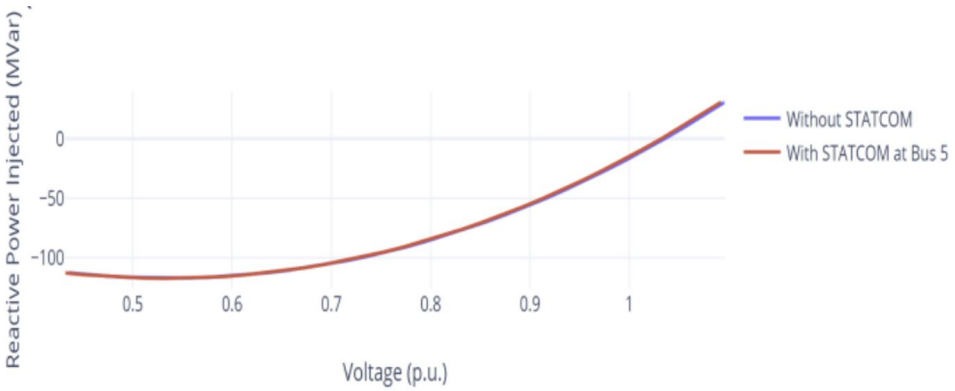

Figure 5.13: QV curves for Bus 5 with wind farm at Bus 5

The table below presents the result for the QV margins of bus when the 100 MW wind farm is connected at its terminal.

Table 5.9: VQ stability margin bus 5 for wind farm power variations

Wind Penetration Level	**QV Margins**
0%	596.54 MVar
60 %	629.62 Mvar
80%	637.27 Mvar
100 %	640.24 Mvar

From the results above, the addition of the wind farm to either the strongest or the weakest bus of the transmission grid improves the QV margins of the transmission grid.

Table 5.10: Comparison of Results

Wind Farm location	**Test bus**	**QV Stability Margin**		
		60 MW	**80 MW**	**100 MW**
14	14	146.34 Mvar	150.48 Mvar	155.35 Mvar
5	5	629.62 Mvar	637.27 Mvar	640.24 Mvar
5	14	117.91 Mvar	118.01 Mvar	118.11 Mvar

5.1.11 Maximum Wind Penetration at bus 14, and 5

Thorough approaches are needed during the planning and the development stages of new a wind farm. The stability of the region cannot be ignored. Furthermore, the maximum wind power that can be transferred under the constraint of keeping the power system voltage stable needs to be considered. For the system under investigation in this work, an iterative approach is used to assess the security of the power system at different wind penetration levels. In addition, the safe P-Q regions of the power system are computed during this iteration process. The tested power levels of the wind farm: 100 MW, 200 MW, 400 MW, and 590 MW. The voltage stability boundary limit is computed each time. Table 5.11 presents the maximum wind power at bus 14 assessed using the P-Q method.

Table 5.11: Stability Limits on Maximum Wind Injection from Bus 14

Wind Penetration Level	**Stability Margin**
100 MW at 0.95 lagging	155.35 Mvar
200 MW at 095 lagging	163.64 Mvar
400 MW at 0.95 lagging	120.89 Mvar
600 MW at 0.95 lagging	22. 86 Mvar
630 MW at 0.95 lagging	Voltage collapse

Table 5.11 demonstrates that the maximum power that can be injected into the system is 100 MW at a power factor of 0.95 lagging. The P-Q regions method has been invoked to compute the maximum wind power that can be reliably integrated at bus 14 of the power system. The results show that around 600 MW the system is on the verge of going into instability. More precisely, at 630 MW the system enters into instability. As a result, the voltage collapse since the system cannot meet its reactive power demand.

The newly installed 100 MW wind farm will be connected to bus 5 of the transmission grid and the maximum wind penetration level is computed using the P-Q regions method.

Table 5.12: Stability Limits on Maximum Wind Injection from Bus 5

Wind Penetration Level	**Stability Margin**
1600 MW at 0.95 lagging	406.70 Mvar
1700 MW at 095 lagging	300.40 Mvar
1800 MW at 0.95 lagging	187.44 Mvar
1900 MW at 0.95 lagging	66. 97 Mvar
2000 MW at 0.95 lagging	Voltage collapse

As can be seen, from table 5.12, the maximum power that can be injected into bus 5 is around 2000 MW. Beyond this amount of power, the system enters into instability and the system voltage decays rapidly until its collapse point. By using the P-Q method analysis, the stability margins of the strongest bus and the weakest are impacted as the wind penetration level augments. However, a higher amount of wind power can be integrated at the strongest bus of the power system with the wind farm connected at the strongest bus. The explanation behind this observation is the connection of the wind farm at the strongest bus has little impact on the eigenvalue of the reduced Jacobian of the power grid. In other words, the critical eigenvalues of the system were insensitive to the amount of wind power at bus 5, the strongest bus of the transmission grid until the high penetration level drives the system into voltage collapse.

To check if the power system is secure in the even of the worst contingency, the line 13 to 14 is open the QV margin stability of the system is computed. For the weakest bus of the system, bus 14, the most severe contingency are the outages of lines 9-14 and line 13-14. Consideration of all possible contingencies might be practical to consider. The dispatcher needs to check for the reliability and the safe operation of the power system. They make periodic calculations to assess the reliability of the system. During these contingencies, the power system should be able to operate safely and reliably. The Steady-state voltage stability analytical P-Q method is used to compute the stability limits bus.

The effects of these contingencies on the voltage stability margins of bus 14 are illustrated in the tables below.

Table 5.13: Stability Limits for Bus 14 with line 6-13 outage

Wind Penetration Level	**Stability Margin**
100 MW at 0.95 lagging	121.6 Mvar
200 MW at 095 lagging	93.57 Mvar
300 MW at 0.95 lagging	97.81 Mvar
400 MW at 0.95 lagging	30. 397 Mvar
600 MW at 0.95 lagging	Voltage collapse

Table 5.14: Stability Limits for Bus 14 with line 13-14 outage

Wind Penetration Level	**Stability Margin**
100 MW at 0.95 lagging	85.98 Mvar
200 MW at 095 lagging	67.77 Mvar
300 MW at 0.95 lagging	21.57 Mvar
400 MW at 0.95 lagging	Voltage collapse

The results in tables 5.13 and 5.14 clearly show that the power system is on the verge of going on voltage collapse with the outages of lines 13-14 and 9-14. The wind power production might need to be curtailed to avoid the voltage collapse of the system.

Chapter 6

Conclusions and Future Works

Wind energy is changing and will continue to change the landscape of the power industry worldwide. The total installed wind power in the world in 2019 worldwide represents 19% of the world installed power. Beyond any doubt, this percentage is going to increase considering the goals of the federal government goals to achieve 20% of wind energy penetration by 2030. With the deployment of these large wind farms into the transmission grid, it is important to research their impacts on the stable operation of a wind-dominated power system.

The deployment of these wind farms causes several problems confronted by grid operators. Existing works in the realm of power operation claim that the deployment of these wind power plants into the grid can be detrimental to voltage stability in all aspects. By performing a literature survey, several gaps have been identified related to this topic. This thesis has attempted to present a systematic approach to connecting large wind farms into a traditional power system considering its strength through modal analysis.

In the first part of the thesis, emphasis has been placed on the behavior of the DFIG with a short-circuit at the point of common coupling of the wind farm with the transmission grid. In this situation, additional reactive power compensation was necessary to satisfy the reactive power of the system. The well-known and sophisticated FACTS device called STATCOM has been used for dynamic reactive power support.

The STATCOM has greatly ameliorated the transient stability during a short-circuit at the point of interconnection to the grid. Furthermore, during the LVRT, the large-scale wind farm has met the grid code requirements with the STATCOM attached to bus 14. SSSC, one of the key FACTS devices, has been used to ameliorate

the Critical Clearing Time when different fault scenarios have been envisaged at some bus of the systems. The results have shown that the SSSC can increase the CCT of the system; hence, can improve the stability. The cost of the most popular FACTS devices has been presented to intuitively approximate the cost of each solution proposed.

The computation of the transmission voltage stability limits has been done via steady-state voltage analytical methods P-V, and Q-V. P-V and Q-V methods could tell the Transmission System Operator, with good approximation, the closeness of the system to the instability point. When the interest is the reactive power variation, the Q-V method is more suitable; otherwise, the P-V method is used if the real power variation is the focus. A combination of these two methods named P-Q methods was used to the power system in this thesis to compute the maximum loading of a particular bus.

There is a close relationship between the strength of the power system and the voltage its voltage security. In the next stage of the steady-state voltage analysis, the QV -modal analysis was invoked to detect the weak and the strong area of the power system under investigation. The Q-V modal analysis is a more precise method for voltage instability prediction in comparison to other static voltage stability methods.

This research has developed a systematic approach to integrating large-scale wind farms into an existing transmission grid by combining the Q-V modal analysis, PV, and QV curves with the P-Q method.

- The voltage stability of the wind-dominated power system was greatly improved by using the STATCOM and the SSSC.
- The P-Q method helped to derive the maximum size of the wind farm during each scenario.
- The integration of the wind to the strongest bus of the power system led to the greater addition of wind power. Conversely, the addition of the wind farm at the weakest bus of the power system limits the amount the quantity of wind

power that can be injected into the power system in comparison to the weakest bus.

- To meet its loads reliably, a power system needs to survive the worst contingencies. Therefore, the system needs to be designed so that the worst contingencies do not drive the power system into voltage collapse. A systematic approach for integrating the wind farm into the transmission grid considering the worst contingencies has been presented.

Future works might focus on the power quality issues related to the use of these power electronics-based devices in the system. Also, techniques to mitigate these issues might be an area of research so that the large could meet the IEEE 1547 standard for interconnection. The study was done using DFIGs but one can include other wind turbine types and use a larger transmission grid to replicate the results. Also, a more rigorous method to detect the worst-case contingency in the power system needs to be researched since it is impractical and unrealistic to consider all possible contingencies.

Publications Arising from the Work Presented in this Thesis

1. Techno-Economic Assessment of Voltage Stability Improvement Using SSSC and STATCOM in a Wind-Dominated Power System, 2021 IEEE Kansas Power and Energy Conference (KPEC)
2. Power Quality Performance on a Feasible Design of a Photovoltaic (PV) Sytem for a Local Community, International Journal of Engineering Research Technology (IJERT)
3. Grid Strength Assessment and Maximum Loadability of a Wind-Dominated Power System Through QV Modal Analysis, IEEE PowerÀfrica Conference 2021.
4. Power System Stabilization of a Grid Highly Penetrated from a Variable-Speed Wind Based Farm Through Robust Means of STATCOM and SSSC," 2021 16th International Conference on Engineering of Modern Electric Systems (EMES)

Bibliography

[1] REN21 Steering Committee. Renewables 2016- global status report. Technical report, REN21, 2016.

[2] Wind in power- 2015 European statistics. Technical report, The European Wind Energy Association, 2016.

[3] E. Vittal, M. O'Malley, and A. Keane. A steady-state voltage stability analysis of power systems with high penetrations of wind. IEEE Transaction on Power System., 25(1):433-442, Feb 2010.

[4] D. Gautam, V. Vittal, and T. Harbour. Impact of increased penetration of DFIG-based wind turbine generators on transient and small signal stability of power systems. IEEE Transaction on Power System., 24(3):1426-1434, 2009

[5] P. Kundur, J. Paserba, V. Ajjarapu, G. Andersson, A. Bose, C. Canizares, N. Hatziargyriou, D. Hill, A. Stankovic, C. Taylor, T. Van Cutsem, and V. Vittal. Definition and classification of power system stability ieee/cigre joint task force on stability terms and definitions. IEEE Transaction on Power System., 19(3):1387-1401, 2004.

[6] T. Sun, Z. Chen, F. Blaabjerg, “Voltage recovery of grid-connected wind turbines with DFIG after a short-circuit fault,” 2004 IEEE 35th Annual Power Electronics Specialists Conference, vol. 3, pp. 1991-97, 20-25 June 2004.

[7] "Wind Energy - The Facts - Executive Summary," Global Wind Energy Council (GWEC), 2009.

[8] Y. Chi, Y. Liu, W. Wang and H. Dai, "Voltage Stability Analysis of Wind Farm Integration into Transmission Network," 2006 International Conference on Power System Technology, 2006, pp. 1-7, doi: 10.1109/ICPST.2006.321661.

[9] Turbine components, http:// www.mstudioblackboard.tudelft.nl/duwind, November 2016.

[10] Wind turbine, https://www.au.mathworks.com, November 2016.

[11] A. Ellis and E. Muljadi, “Wind Power Plant Representation in Large-Scale Power Flow Simulations in WECC”, in 2008 IEEE Power and Energy Society General Meeting Conversion and delivery of Electrical Energy in the Century, 2008, pp. 1-6, pp. 1-6, 2008.

[12] Heping Zou, Hui Sun, Jiyan Zou, “Fault Ride-through Performance of Wind Turbine with Doubly Fed Induction Generator,” 2nd IEEE Conference on Industrial Electronics and Applications, pp. 1607-11, 23-25 May 2007.

[13] Ahmed G. Abo-Khalil (March 20th 2013). Impacts of Wind Farms on Power System Stability, Modeling and Control Aspects of Wind Power Systems, S. M. Muyeen, Ahmed Al-Durra and Hany M. Hasanien, IntechOpen, DOI: 10.5772/55090.

[14] Hill, D., 1993. Nonlinear dynamic load models with recovery for voltage stability studies. IEEE Transactions on Power Systems, 8(1), pp.166-176.

[15] Borghetti, A., Caldon, R., Mari, A. and Nucci, C., 1997. On dynamic load models for voltage stability studies. IEEE Transactions on Power Systems, 12(1), pp.293-303.

[16] Federal Energy Regulatory Commission (FERC), United States of America, Docket No. RM05-4-001; Order No. 661-A, "Interconnection for Wind Energy," Issued December 12, 2005.

[17] V. S. Sravan Kumar, K. Krishna Reddy, and D. Thukaram. Coordination of reactive power in grid-connected wind farms for voltage stability enhancement. IEEE Transaction on Power System., 29(5):2381-2390, Sept 2014.

[18] Carson W. Taylor. Power System Voltage Stability. McGRAW-Hill, Inc., 1994.

[19] Kundur, Prabha. Power system stability and control. Tata McGraw-Hill Education, 1994.

[20] T. Van Cutsem. Voltage instability: phenomena, countermeasures, and analysis methods. Proceedings of the IEEE, 88(2):208-227, Feb 2000.

[21] T. Van Cutsem. Voltage instability: phenomena, countermeasures, and analysis methods. Proceedings of the IEEE, 88(2):208-227, Feb 2000.

[22] Van Cutsem, T., 2000. Voltage instability: phenomena, countermeasures, and analysis methods. Proceedings of the IEEE, 88(2), pp.208-227.

[23] V. Ajjarapu and C. Christy. The continuation power ¸ow: a tool for steady state voltage stability analysis. IEEE Transaction on Power System., 7(1):416-423, 1992.

[24] Gao, B., G. K. Morison, and P. Kundur. "Towards the development of a systematic approach for voltage stability assessment of large-scale power systems." IEEE Transactions on Power Systems 11.3 (1996): 1314-1324.

[25] Gao, Baofu, G. K. Morison, and Prabhashankar Kundur. "Voltage stability evaluation using modal analysis." IEEE Transactions on Power Systems 7.4 (1992): 1529-1542.

[26] F. M. Hughes, O. Anaya-Lara, N. Jenkins, and G. Strbac, "Control of dfg-based wind generation for power network support," IEEE Transactions on Power Systems, vol. 20, no. 4, pp. 1958-1966, 2005.

[27] Lund, T., Sørensen, P. and Eek, J., 2007. Reactive power capability of a wind turbine with doubly fed induction generator. Wind Energy, 10(4), pp.379-394.

[28] S. Engelhardt, I. Erlich, C. Feltes, J. Kretschmann, and F. Shewarega, "Reactive power capability of wind turbines based on doubly fed induction generators," IEEE Transactions on Energy Conversion, vol. 26, no. 1, pp. 364-372, 2011.

[29] H. A. Pulgar-Painemal and P. W. Sauer, "Doubly-fed induction machine in wind power generation," in Electrical Manufacturing and Coil Winding Exposition, 2009.

[30] I. A. Pecas, F. P. Maciel, and I. CidrAs, "Simulation of MV distribution networks with asynchronous local generation sources, Proceeding in IEEE Melecom 91, June 1991.

[31] Cidrás, J., Martinez-Velasco, J., Peças Lopes, J. and Maciel Barbosa, F., 1992. Modelling of Nonlinear Nodal Admittances in Load Flow Analysis. IFAC Proceedings Volumes, 25(1), pp.245-249.

[32] Vittal, E., O'Malley, M. and Keane, A., 2012. Rotor Angle Stability with High Penetrations of Wind Generation. IEEE Transactions on Power Systems, 27(1), pp.353-362.

[33] K. Burges and J. Twele, "Power systems operation with high penetration of renewable energy - the German case," 2005.

[34] Lee, H., Bae, M. and Lee, B., 2017. Advanced Reactive Power Reserve Management Scheme to Enhance LVRT Capability. Energies, 10(10), p.1540.

[35] J. D. Glover, T. J. Overbye, and M. S. Sarma, Power system analysis amp; design. 2017.

[36] Saad-Saoud, Z., Lisboa, M., Ekanayake, J., Jenkins, N. and Strbac, G., 1998. Application of STATCOMs to wind farms. IEE Proceedings - Generation, Transmission and Distribution, 145(5), p.511.

[37] N.G. Hingorani, L. Gyugyi, Understanding FACTS: Concepts and Technology of Flexible AC Transmission Systems, New York, Wiley-IEEE Press, 1999.

[38] E. Muljadi et al., "Equivalencing the collector system of a large wind power plant," IEEE Power Engineering Society General Meeting, 2006, pp. 9 pp.-, doi: 10.1109/PES.2006.1708945.

[39] T. Sun, Z. Chen and F. Blaabjerg, "Voltage recovery of grid-connected wind turbines with DFIG after a short-circuit fault," IEEE 35th Annual Power Electronics Specialists Conference (IEEE Cat. No.04CH37551), 2004, pp. 1991-1997 Vol.3, doi: 10.1109/PESC.2004.1355423.

[40] Y. A. KAPLAN, "Determination of Weibull Parameters by Di˙erent Numerical Methods and Analysis of Wind Power Density in Osmaniye, Turkey," Scientia Iranica, 2017.

[41] S. V. Dhople and A. D. Dominguez-Garcia, “A framework to determine the probability density function for the output power of wind farms,” 2012 North American Power Symposium (NAPS), 2012.

[42] K. Alqunun, T. Guesmi, A. F. Albaker, and M. T. Alturki, “Stochastic Unit Commitment Problem, Incorporating Wind Power and an Energy Storage System,” Sustainability, vol. 12, no. 23, p. 10100, 2020.

[43] T. Ackermann, Wind power in power systems. Chichester, West Sussex: Wiley, 2012.

[44] A. M. Ghani, R. E. Fehr, E. K. Stefanakos, and W. Moreno, “Improving stability by enhancing critical fault clearing time,” dissertation.

[45] Daneshi, H.; Srivastava, A.K. Security-constrained unit commitment with wind generation and compressed air energy storage. IET Gener. Transm. Distrib. 2012, 6, 167-175

[46] Nikolaidis, P.; Chatzis, S.; Poullikkas, A. Renewable energy integration through optimal unit commitment and electricity storage in weak power networks. Int.J. Sustain. Energy 2019, 38, 398-414

[47] Morales-Espana, G.; Lorca, A.; de Weerdt, M.M. Robust unit commitment with dispatchable wind power. Electr. Power Syst. Res. 2018, 155, 58-66

[48] S. Gandhar, J. Ohri, and M. Singh, “Application of SSSC for compensation as-sessment of interconnected Power System,” 2014, IEEE 6th India International Conference on Power Electronics (IICPE), 2014.

[49] K. Habur and D. O'Leary, "FACTS - for cost effective and reliable transmission of electrical energy," .

[50] Honrubia-Escribano, A., Gómez-Lázaro, E., Fortmann, J., Sørensen, P. and Martin-Martinez, S., 2018. Generic dynamic wind turbine models for power system stability analysis: A comprehensive review. Renewable and Sustainable Energy Reviews, 81, pp.1939-1952.

[51] P. O. Dorile, D. R. Jagessar and R. A. McCann, "Techno-Economic Assessment of Voltage Stability Improvement Using SSSC and STATCOM in a Wind-Dominated Power System," 2021 IEEE Kansas Power and Energy Conference (KPEC), 2021, pp. 1-6, doi: 10.1109/KPEC51835.2021.9446260.

[52] P. O. Dorile, D. R. Jagessar, L. Guardado, S. S. Jagessar and R. A. McCann, "Power System Stabilization of a Grid Highly Penetrated from a Variable-Speed Wind Based Farm Through Robust Means of STATCOM and SSSC," 2021 16th International Conference on Engineering of Modern Electric Systems (EMES), 2021, pp. 1-6, doi: 10.1109/EMES52337.2021.9484110.